

Ethylene Insertion and β -Hydrogen Elimination for Permethylscandocene Alkyl Complexes. A Study of the Chain Propagation and Termination Steps in Ziegler-Natta Polymerization of Ethylene

Barbara J. Burger,¹ Mark E. Thompson,² W. Donald Cotter, and John E. Bercaw*

Contribution No. 7948 from the Division of Chemistry and Chemical Engineering, California Institute of Technology, Pasadena, California 91125. Received May 5, 1989

Abstract: The rates of ethylene insertion into the Sc-C bond for Cp^*_2ScR ($\text{Cp}^* = (\eta^5\text{-C}_5\text{Me}_5)$, $\text{R} = \text{CH}_3, \text{CH}_2\text{CH}_3, \text{CH}_2\text{CH}_2\text{CH}_3$) have been measured at -80°C by ^{13}C NMR; the second order rate constants ($\text{M}^{-1}\text{s}^{-1}$) are as follows: $\text{R} = \text{CH}_3$, $8.1 (2) \times 10^{-4}$; $\text{R} = \text{CH}_2\text{CH}_3$, $4.4 (2) \times 10^{-4}$; $\text{R} = \text{CH}_2\text{CH}_2\text{CH}_3$, $6.1 (2) \times 10^{-3}$. The slow rate for the ScCH_2CH_3 complex is attributed to a ground-state stabilization by a $\beta\text{-C-H}$ "agostic" interaction. The distributions of molecular weights for ethylene oligomers ($\text{CH}_3(\text{CH}_2)_n\text{CH}_3$, $n = 11-47$) produced from known amounts of ethylene and $\text{Cp}^*_2\text{ScCH}_2\text{CH}_2\text{CH}_3$ at -80°C satisfactorily fit a Poisson distribution, indicative of a "living" Ziegler-Natta polymerization system. From the measured, slower initiation rates of insertion for $\text{Cp}^*_2\text{ScCH}_3$ and $\text{Cp}^*_2\text{ScCH}_2\text{CH}_3$ and propagation rates equal to that for $\text{Cp}^*_2\text{ScCH}_2\text{CH}_2\text{CH}_3$, the molecular weight distributions of ethylene oligomers are also accurately predicted. $\text{Cp}^*_2\text{ScCH}_3$ undergoes a single insertion with 2-butyne with a moderate enthalpy of activation and a large, negative entropy of activation. The second-order rate constants for the insertion of 3-phenyl-2-propyne, 2-pentyne, and 4-methyl-2-pentyne have been measured. The rates for β -hydrogen elimination for members of the series of permethylscandocene alkyl complexes $\text{Cp}^*_2\text{ScCH}_2\text{CH}_2\text{R}$ ($\text{R} = \text{H}, \text{CH}_3, \text{CH}_2\text{CH}_3, \text{C}_6\text{H}_5, \text{C}_6\text{H}_4\text{-}p\text{-CH}_3, \text{C}_6\text{H}_4\text{-}p\text{-CF}_3, \text{C}_6\text{H}_4\text{-}p\text{-NMe}_2$) have been obtained by rapidly trapping Cp^*_2ScH with 2-butyne. A transition state for the β -hydrogen elimination is indicated with partial charge on the β -carbon. Hydrogen is thus transferred to the scandium center as hydride in the β -H elimination process.

Olefin insertion into metal-carbon bonds and β -hydrogen elimination are fundamental transformations that occur in a variety of organometallic systems.^{3,4} Indeed, at least one of these reactions is an essential step in virtually all catalytic cycles involving olefins. For olefin polymerization, chain propagation occurs by olefin insertion into a metal-carbon bond while β -hydrogen elimination serves as a chain-termination ("chain-transfer") step. Normally, it is the relative rates of these two steps that determine the chain length of the polymer.⁵

The recent work of Watson,⁶ Eisch, Jordan,⁸ Marks,⁹ and Grubbs¹⁰ provides compelling support for olefin insertion into the metal-alkyl bond as the mode of propagation in Ziegler-Natta polymerization of ethylene and other olefins (the Cossee-Arlman mechanism), at least for catalysts based on d^0 transition and d^{0f} lanthanide metals.¹¹ Efforts to gain further insight into the mechanism and the factors affecting the rate of the actual olefin insertion step have been met with limited success, however. Unlike carbon monoxide, which undergoes a single insertion, most olefins

undergo multiple insertions to form oligomers and polymers, thus complicating the kinetic scheme. Moreover, in most cases the rates are exceedingly fast, approaching diffusion controlled, and the catalytically active species is ill-defined so that its identity and concentration are unknown.¹² Although previous studies have shown that the rate of insertion varies markedly with the nature of the olefin (the more substituted the olefin, the less reactive: i.e., ethylene \gg propene $>$ 1-butene $>$ 2-butene),¹³ the stereoelectronic factors dictating this order are not yet understood. Furthermore, little is known about the effect that the alkyl group (the migrating group) has on the rate of olefin insertion.

The factors governing the rate of β -H elimination, "chain transfer", in these catalytic systems are also poorly understood. In addition to being a termination path for olefin polymerization, β -hydrogen elimination is a common decomposition route for metal alkyls; indeed, the facility of this pathway often precludes isolation of stable alkyl complexes with β -hydrogens. As with the olefin insertion reaction, β -hydrogen elimination often is not rate limiting and, as such, is difficult to study mechanistically, since other reactions complicate the kinetic scheme.¹⁴ As shown by Whitesides,¹⁵ thermal extrusion of a ligand from a coordinatively saturated complex generally requires higher temperatures than β -hydrogen transfer. In some cases, rate-limiting formation of the coordinatively unsaturated species can be circumvented by photochemically dissociating a ligand.¹⁶ Due to the difficulties described with isolating the β -hydrogen elimination reaction, there has been no systematic study done to date that has addressed steric and electronic effects. A better understanding of these processes could aid in the design of new catalysts capable of producing polymers with controlled molecular weight distributions as well as in developing new "living" and block polymerization systems.

(1) Present address: Chevron Research Co., P.O. Box 1627, Richmond, CA 94802-0627.

(2) Present address: Department of Chemistry, Princeton University, Princeton, NJ 08544.

(3) Parshall, G. W. *Homogeneous Catalysis*; John Wiley & Sons: New York, 1980; Chapter 3.

(4) For a general review of β -elimination reactions, see: Cross, R. J. In *The Chemistry of the Metal-Carbon Bond*; Hartley, F. R., Patia, S., Eds.; John Wiley and Sons: New York, 1985; Vol. 2, Chapter 8.

(5) Collman, J. P.; Hegedus, L. S.; Norton, J. R.; Finke, R. G. *Principles and Applications of Organometallic Chemistry*; University Science Books: Mill Valley, CA, 1987; p 567.

(6) (a) Watson, P. L. *J. Am. Chem. Soc.* **1982**, *104*, 337-339. (b) Watson, P. L.; Roe, D. C. *J. Am. Chem. Soc.* **1982**, *107*, 6471-6473.

(7) Eisch, J. J.; Piotrowski, A. M.; Brownstein, S. K.; Gabe, E. J.; Lee, F. L. *J. Am. Chem. Soc.* **1985**, *107*, 7219-7221.

(8) (a) Jordan, R. F.; Dasher, W. E.; Echols, S. F. *J. Am. Chem. Soc.* **1986**, *108*, 1718-1719. (b) Jordan, R. F.; Bajgur, C. S.; Willett, R.; Scott, B. *J. Am. Chem. Soc.* **1986**, *108*, 7410-7411.

(9) Jeske, G.; Lauke, H.; Mauermann, H.; Swepston, P. N.; Schumann, H.; Marks, T. J. *J. Am. Chem. Soc.* **1985**, *107*, 8091.

(10) (a) Soto, J.; Steigerwald, M. L.; Grubbs, R. H. *J. Am. Chem. Soc.* **1982**, *104*, 4479. (b) Clawson, L.; Soto, J.; Buchwald, S. L.; Steigerwald, M. L.; Grubbs, R. H. *J. Am. Chem. Soc.* **1985**, *107*, 3377-3378.

(11) (a) Cossee, P. *J. Catal.* **1964**, *3*, 80. (b) Arlman, E. J.; Cossee, P. *J. Catal.* **1964**, *3*, 99.

(12) Gates, B. C.; Katzer, J. R.; Schuit, G. C. A. *Chemistry of Catalytic Processes*; McGraw-Hill: New York, 1979; p 150.

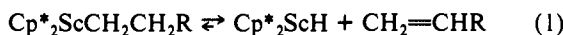
(13) Reference 3, p 578.

(14) (a) Doherty, N. M.; Bercaw, J. E. *J. Am. Chem. Soc.* **1985**, *107*, 2670. (b) Burger, B. J.; Santarsiero, B. D.; Trimmer, M. S.; Bercaw, J. E. *J. Am. Chem. Soc.* **1988**, *110*, 3134.

(15) Whitesides, G. M.; Gaasch, J. F.; Stedronsky, E. R. *J. Am. Chem. Soc.* **1972**, *94*, 5258-5270.

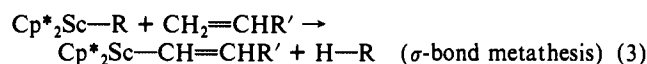
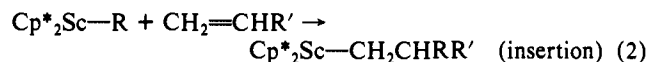
(16) Kazlauskas, R. J.; Wrighton, M. S. *J. Am. Chem. Soc.* **1982**, *104*, 6005-6015.

Recent efforts in our research group have focused on the synthesis and reactivity of alkyl complexes of permethylscandocene, Cp^*_2ScR [$\text{Cp}^* = (\eta^5\text{-C}_5\text{Me}_5)$].¹⁷ Permethylscandocene alkyl complexes with β -hydrogens have been prepared and appear to be moderately stable in solution.^{17c} They are, however, coordinatively unsaturated and, as such, could decompose by formation of a scandium hydride complex and liberation of olefin (olefin adducts for a d^0 metal center are not expected to be stable and have not been directly observed). Although β -hydrogen elimination has been predicted to be thermodynamically unfavorable in d^0 and d^0m systems¹⁸ (eq 1), it could, nonetheless, be kinetically



significant. Indeed, evidence from our studies of ethylene polymerization (vide infra) suggests that β -H elimination is a major termination pathway for this reaction.¹⁹

These permethylscandocene alkyl complexes have been shown to react with olefins by two distinct routes (eq 2 and 3). Insertion



of olefin into the Sc-C bond (eq 2) occurs for all scandium alkyl and aryl complexes when the olefin is ethylene, and for the scandium methyl complex when the olefin is propene (multiple insertions of ethylene are observed; a single insertion is observed with propene). For all other olefins, the σ -bond metathesis pathway is preferred, producing a scandium alkenyl complex and free alkane.

Due to the steric bulk of the pentamethylcyclopentadienyl ligands permethylscandocene alkyl complexes are monomeric and can be prepared free of coordinating solvent. They smoothly insert ethylene in the absence of any Lewis acid cocatalysts, thus providing a rare opportunity to examine in situ a functioning ethylene polymerization catalyst. Since ethylene insertion proceeds cleanly at -80°C , and β -H elimination (chain transfer) occurs at much higher temperatures ($>0^\circ\text{C}$), the kinetics of these two processes may be isolated from one another. A series of alkyl complexes of permethylscandocene, including para-substituted phenethyl complexes, have been prepared in order to probe the steric and electronic factors of the β -hydrogen elimination reaction. The effect of the migrating alkyl group on the olefin insertion rate has been probed by measuring the ethylene insertion rate for a series of permethylscandocene alkyl complexes by ^{13}C NMR spectroscopy at -80°C . In addition, the stoichiometric reaction of scandium alkyl complexes with internal alkynes has been investigated as a model for a single insertion in the ethylene polymerization reaction. In principle, molecular weight distributions for oligo- or polyethylenes should be predictable from these relative rates of ethylene insertion. Accordingly, oligoethylenes have been prepared via treatment of Cp^*_2ScR ($\text{R} = \text{CH}_3, \text{CH}_2\text{CH}_3, \text{CH}_2\text{CH}_2\text{CH}_3$) with ethylene at -80°C and their compositions compared to those predicted.

Results

Ethylene Insertion Reactions with Permethylscandocene Alkyl Complexes. Second-order rate constants for ethylene insertion into the Sc-C bond of Cp^*_2ScR ($\text{R} = \text{CH}_3, \text{CH}_2\text{CH}_3,$

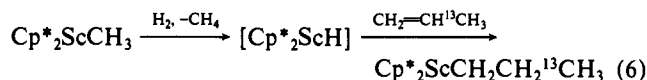
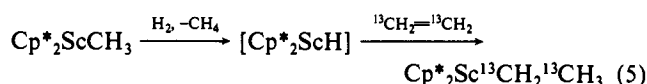
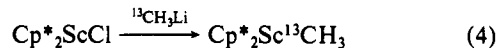
 Table I. ^1H NMR Data^a

compound	assignment	δ , ppm	coupling, Hz
$\text{Cp}^*_2\text{ScCH}_2\text{CH}_2\text{CH}_2\text{CH}_3$ ^b	$[\text{C}_5(\text{CH}_3)_5]$	1.88 (s)	
	$\alpha\text{-CH}_2$	0.90 (t)	$J_{\text{HH}} = 7.44$
	$\beta, \gamma, \delta\text{-CH}_2(3)$	0.56–0.61 (m)	
	$[\text{C}_5(\text{CH}_3)_5]$	1.84 (s)	
$\text{Cp}^*_2\text{ScCH}_2\text{CH}_2\text{C}_6\text{H}_5$ ^c	$\text{CH}_2\text{CH}_2\text{C}_6\text{H}_5$	1.01 (m)	AA'BB'
	$\text{CH}_2\text{CH}_2\text{C}_6\text{H}_5$	2.38 (m)	AA'BB'
	$\text{CH}_2\text{CH}_2\text{C}_6\text{H}_5$	7.48 (d)	$^3J_{\text{HH}} = 7.0$
	$\text{CH}_2\text{CH}_2\text{C}_6\text{H}_5$	7.30 (d)	$^3J_{\text{HH}} = 8.0$
	$\text{CH}_2\text{CH}_2\text{C}_6\text{H}_5$	7.124 (t)	$^3J_{\text{HH}} = 7.5$
	$[\text{C}_5(\text{CH}_3)_5]$	1.89 (s)	
	$\text{CH}_2\text{CH}_2\text{C}_6\text{H}_4$	1.11 (m)	AA'BB'
$\text{Cp}^*_2\text{ScCH}_2\text{CH}_2\text{C}_6\text{H}_4$ ^b <i>p</i> -NMe ₂	$\text{CH}_2\text{CH}_2\text{C}_6\text{H}_4$	2.27 (m)	AA'BB'
	$\text{CH}_2\text{CH}_2\text{C}_6\text{H}_4$	7.04 (d)	$^3J_{\text{HH}} = 8.5$
	$\text{CH}_2\text{CH}_2\text{C}_6\text{H}_4$	6.57 (d)	$^3J_{\text{HH}} = 8.5$
	$\text{N}(\text{CH}_3)_2$	2.82 (s)	
	$[\text{C}_5(\text{CH}_3)_5]$	1.82 (s)	
	$\text{CH}_2\text{CH}_2\text{C}_6\text{H}_4$	0.84 (m)	AA'BB'
$\text{Cp}^*_2\text{ScCH}_2\text{CH}_2\text{C}_6\text{H}_4$ ^c <i>p</i> -CF ₃	$\text{CH}_2\text{CH}_2\text{C}_6\text{H}_4$	2.38 (m)	AA'BB'
	$\text{CH}_2\text{CH}_2\text{C}_6\text{H}_4$	7.48 (d)	$^3J_{\text{HH}} = 8.0$
	$\text{CH}_2\text{CH}_2\text{C}_6\text{H}_4$	7.35 (d)	$^3J_{\text{HH}} = 8.0$
	$[\text{C}_5(\text{CH}_3)_5]$	1.85 (s)	
$\text{Cp}^*_2\text{ScCH}_2\text{CH}_2\text{C}_6\text{H}_4$ ^b <i>p</i> -CH ₃	$\text{CH}_2\text{CH}_2\text{C}_6\text{H}_4$	1.15 (m)	AA'BB'
	$\text{CH}_2\text{CH}_2\text{C}_6\text{H}_4$	2.42 (m)	AA'BB'
	$\text{CH}_2\text{CH}_2\text{C}_6\text{H}_4$	7.19 (d)	$^3J_{\text{HH}} = 7.8$
	$\text{CH}_2\text{CH}_2\text{C}_6\text{H}_4$	7.51 (d)	$^3J_{\text{HH}} = 7.8$
	CH_3	2.25 (s)	
	$[\text{C}_5(\text{CH}_3)_5]$	1.85 (s)	

^a ^1H (90- and 400-MHz) NMR spectra were taken in benzene-*d*₆ at ambient temperature, unless otherwise stated. Chemical shifts are reported in parts per million (δ) from tetramethylsilane added as an internal reference or to residual protons in the solvent. Coupling constants are reported in hertz. ^bCyclohexane-*d*₁₂ at room temperature, 400 MHz. ^cToluene-*d*₈ at room temperature, 400 MHz.

$\text{CH}_2\text{CH}_2\text{CH}_3$) at -80°C have been measured by using ^{13}C NMR spectroscopy, due to its sensitivity to the position of a carbon atom in a hydrocarbon chain.²⁰ Although ^{13}C spectra of polymers and organometallic complexes are routinely obtained by using the natural abundance of ^{13}C (1.1%), acquisition times on the order of an hour are usually required for high-resolution spectra, depending on sample concentration, number of equivalent nuclei, etc. In standard acquisitions, short pulse delays are utilized to achieve maximum signal to noise; all quantitative information (signal intensity as a measure of concentration) is essentially lost, however. In order for quantitative information to be obtained from the spectra, the long carbon translational relaxation times (T_1) require that long pulse delays be employed to ensure adequate relaxation between pulses. Techniques that allow quantitative information to be obtained from ^{13}C NMR spectra have been developed,²¹ but these methods are limited to reactions with very long half-lives with samples of natural-abundance ^{13}C . Thus, the use of ^{13}C -enriched samples was deemed necessary in this system so that spectra with adequate signal to noise could be obtained with a minimum number of acquisitions.

The use of selectively ^{13}C -labeled scandium alkyl complexes and natural-abundance ethylene (1.1% ^{13}C) provides spectra that are readily interpreted. Selectively ^{13}C -labeled scandium alkyl complexes were prepared as shown (eq 4–6); the syntheses of



$\text{Cp}^*_2\text{Sc}^{13}\text{CH}_3$ and $\text{Cp}^*_2\text{Sc}^{13}\text{CH}_2^{13}\text{CH}_3$ have been previously re-

(17) (a) Thompson, M. E.; Bercaw, J. E. *Pure Appl. Chem.* **1984**, *56*, 1. (b) Thompson, M. E. Ph.D. Thesis, California Institute of Technology, 1985. (c) Thompson, M. E.; Baxter, S. M.; Bulls, A. R.; Burger, B. J.; Nolan, M. C.; Santarsiero, B. D.; Schaefer, W. P.; Bercaw, J. E. *J. Am. Chem. Soc.* **1987**, *109*, 203–219. (d) Bulls, A. R.; Manriquez, J. M.; Thompson, M. E.; Bercaw, J. E. *Polyhedron* **1988**, *7*, 1409–1428.

(18) Bruno, J. W.; Marks, T. J.; Morss, L. R. *J. Am. Chem. Soc.* **1983**, *105*, 6824–6832.

(19) The IR spectrum of the polymer obtained from the reaction of $\text{Cp}^*_2\text{ScCH}_3$ and excess ethylene contained bands typical of polyethylene as well as bands characteristic of vinyl groups. Vinyl groups were thought to arise from vinyl groups formed by chain-terminating β -hydrogen elimination. See: Reference 17b.

(20) For a good review on the use of ^{13}C NMR in polymer characterization, see: Randall, J. C. In *Polymer Characterization by NMR and ESR*; Woodward, A. E., Bovey, F. A., Eds.; ACS Symposium Series 142; American Chemical Society: Washington, DC, 1980; Chapter 6.

(21) Shoolery, J. N. *Prog. Nucl. Magn. Reson. Spectrosc.* **1977**, *11*, 79–93.

Table II. ^{13}C NMR Data^a

compound	assignment	δ , ppm (coupling, Hz)
$\text{Cp}^*_2\text{ScCH}_3^b$	$\text{C}_5(\text{CH}_3)_5$	118.92
	$\text{C}_5(\text{CH}_3)_5$	11.14
$\text{Cp}^*_2\text{ScCH}_2\text{CH}_3^b$	ScCH_3	25.36 (br s, $J_{\text{CH}} = 111$)
	$\text{C}_5(\text{CH}_3)_5$	116.78
	$\text{C}_5(\text{CH}_3)_5$	11.89
	ScCH_2CH_3	36.86 (t, $J_{\text{CH}} = 119$)
$\text{Cp}^*_2\text{ScCH}_2\text{CH}_2\text{CH}_3^b$	ScCH_2CH_3	20.46 (q, $J_{\text{CH}} = 120$)
	$\text{C}_5(\text{CH}_3)_5$	118.60
	$\text{C}_5(\text{CH}_3)_5$	11.19
	$\text{ScCH}_2\text{CH}_2\text{CH}_3$	45.8 (t, $J_{\text{CH}} = 117$)
	$\text{ScCH}_2\text{CH}_2\text{CH}_3$	24.58
$\text{Cp}^*_2\text{ScCH}_2\text{CH}_2\text{CH}_2\text{CH}_3^c$	$\text{ScCH}_2\text{CH}_2\text{CH}_3$	22.76
	$\text{C}_5(\text{CH}_3)_5$	119.29
	$\text{C}_5(\text{CH}_3)_5$	11.42
	$\text{ScCH}_2\text{CH}_2\text{CH}_2\text{CH}_3$	43.43
	$\text{ScCH}_2\text{CH}_2\text{CH}_2\text{CH}_3$	30.70
	$\text{ScCH}_2\text{CH}_2\text{CH}_2\text{CH}_3$	34.47
$\text{Cp}^*_2\text{ScCH}_2\text{CH}_2\text{CH}_2\text{CH}_2\text{CH}_3^c$	$\text{ScCH}_2\text{CH}_2\text{CH}_2\text{CH}_3$	14.49
	$\text{C}_5(\text{CH}_3)_5$	119.24
	$\text{C}_5(\text{CH}_3)_5$	11.43
	$\text{ScCH}_2\text{CH}_2\text{CH}_2\text{CH}_2\text{CH}_3$	43.43
	$\text{ScCH}_2\text{CH}_2\text{CH}_2\text{CH}_2\text{CH}_3$	31.73
	$\text{ScCH}_2\text{CH}_2\text{CH}_2\text{CH}_2\text{CH}_3$	40.80
	$\text{ScCH}_2\text{CH}_2\text{CH}_2\text{CH}_2\text{CH}_3$	23.61
	$\text{ScCH}_2\text{CH}_2\text{CH}_2\text{CH}_2\text{CH}_3$	14.69
$\text{Cp}^*_2\text{ScCH}_2\text{CH}_2\text{CH}_2\text{CH}_2\text{CH}_2\text{CH}_3^c$	$\text{C}_5(\text{CH}_3)_5$	119.27
	$\text{C}_5(\text{CH}_3)_5$	11.45
	$\text{ScCH}_2\text{CH}_2\text{CH}_2\text{CH}_2\text{CH}_2\text{CH}_3$	43.96
	$\text{ScCH}_2\text{CH}_2\text{CH}_2\text{CH}_2\text{CH}_2\text{CH}_3$	32.99
	$\text{ScCH}_2\text{CH}_2\text{CH}_2\text{CH}_2\text{CH}_2\text{CH}_3$	32.08
	$\text{ScCH}_2\text{CH}_2\text{CH}_2\text{CH}_2\text{CH}_2\text{CH}_3$	37.70
	$\text{ScCH}_2\text{CH}_2\text{CH}_2\text{CH}_2\text{CH}_2\text{CH}_3$	23.71
	$\text{ScCH}_2\text{CH}_2\text{CH}_2\text{CH}_2\text{CH}_2\text{CH}_3$	14.68
	$\text{C}_5(\text{CH}_3)_5$	119.9 (s)
	$\text{C}_5(\text{CH}_3)_5$	11.47 (q, $J_{\text{CH}} = 125$)
	$\text{ScCH}_2\text{CH}_2\text{C}_6\text{H}_5$	(not located)
	$\text{ScCH}_2\text{CH}_2\text{C}_6\text{H}_5$	36.92 (t, $J_{\text{CH}} = 118.8$)
$\text{ScCH}_2\text{CH}_2\text{C}_6\text{H}_5$	C_1 149.0 (s)	
$\text{ScCH}_2\text{CH}_2\text{C}_6\text{H}_5$	$\text{C}_{2,6}$ 127.76 (d, $J_{\text{CH}} = 165$)	
$\text{ScCH}_2\text{CH}_2\text{C}_6\text{H}_5$	$\text{C}_{3,5}$ 128.23 (d, $J_{\text{CH}} = 161$)	
$\text{ScCH}_2\text{CH}_2\text{C}_6\text{H}_5$	C_4 124.46 (d, $J_{\text{CH}} = 158$)	
$\text{Cp}^*_2\text{ScCH}_2\text{CH}_2\text{C}_6\text{H}_4\text{-}p\text{-NMe}_2^c$	$\text{ScCH}_2\text{CH}_2\text{C}_6\text{H}_5$	119.59 (s)
	$\text{C}_5(\text{CH}_3)_5$	11.50 (q, $J_{\text{CH}} = 124.7$)
	$\text{ScCH}_2\text{CH}_2\text{C}_6\text{H}_4$	(not located)
	$\text{ScCH}_2\text{CH}_2\text{C}_6\text{H}_4$	36.37 (t, $J_{\text{CH}} = 122.5$)
	$\text{ScCH}_2\text{CH}_2\text{C}_6\text{H}_4$	C_1 148.62 (s)
	$\text{ScCH}_2\text{CH}_2\text{C}_6\text{H}_4$	$\text{C}_{2,6}$ 128.14 (d, $J_{\text{CH}} = 151.9$)
	$\text{ScCH}_2\text{CH}_2\text{C}_6\text{H}_4$	$\text{C}_{3,5}$ 113.44 (d, $J_{\text{CH}} = 154.1$)
	$\text{ScCH}_2\text{CH}_2\text{C}_6\text{H}_4$	C_4 137.35 (s)
	$\text{ScCH}_2\text{CH}_2\text{C}_6\text{H}_4\text{N}(\text{CH}_3)_2$	41.36 (q, $J_{\text{CH}} = 125.2$)
	$\text{C}_5(\text{CH}_3)_5$	120.30 (s)
$\text{Cp}^*_2\text{ScCH}_2\text{CH}_2\text{C}_6\text{H}_4\text{-}p\text{-CF}_3^c$	$\text{C}_5(\text{CH}_3)_5$	11.42 (q)
	$\text{ScCH}_2\text{CH}_2\text{C}_6\text{H}_4$	(not located)
	$\text{ScCH}_2\text{CH}_2\text{C}_6\text{H}_4$	36.50 (t)
	$\text{ScCH}_2\text{CH}_2\text{C}_6\text{H}_4$	(not located)
	$\text{ScCH}_2\text{CH}_2\text{C}_6\text{H}_4$	C_1 (not located)
	$\text{ScCH}_2\text{CH}_2\text{C}_6\text{H}_4$	$\text{C}_{2,6}$ 127.69
	$\text{ScCH}_2\text{CH}_2\text{C}_6\text{H}_4$	$\text{C}_{3,5}$ 124.91
	$\text{ScCH}_2\text{CH}_2\text{C}_6\text{H}_4$	C_4 124.87
	CF_3	(not located)
	$\text{C}_5(\text{CH}_3)_5$	119.84 (s)
$\text{Cp}^*_2\text{ScCH}_2\text{CH}_2\text{C}_6\text{H}_4\text{-}p\text{-CH}_3^c$	$\text{C}_5(\text{CH}_3)_5$	11.49 (q, $J_{\text{CH}} = 124.9$)
	$\text{ScCH}_2\text{CH}_2\text{C}_6\text{H}_4$	42.67 (t, $J_{\text{CH}} = 116.3$)
	$\text{ScCH}_2\text{CH}_2\text{C}_6\text{H}_4$	36.57 (t, $J_{\text{CH}} = 118.1$)
	$\text{ScCH}_2\text{CH}_2\text{C}_6\text{H}_4$	C_4 145.92 (s)
	$\text{ScCH}_2\text{CH}_2\text{C}_6\text{H}_4$	$\text{C}_{2,6}$ 127.59 (d, $J_{\text{CH}} = 152.6$)
	$\text{ScCH}_2\text{CH}_2\text{C}_6\text{H}_4$	$\text{C}_{3,5}$ 128.51 (d, $J_{\text{CH}} = 159.9$)
	$\text{ScCH}_2\text{CH}_2\text{C}_6\text{H}_4$	C_4 133.21 (s)
	$\text{ScCH}_2\text{CH}_2\text{C}_6\text{H}_4\text{CH}_3$	21.29 (q, $J_{\text{CH}} = 124.9$)

^a ^{13}C (100.25-MHz) NMR spectra were taken in benzene- d_6 at ambient temperature, unless otherwise stated. Chemical shifts are reported in parts per million (δ) from tetramethylsilane referenced from solvent signal. Coupling constants ($J_{^{13}\text{C}-^1\text{H}}$) were obtained from a gated (^1H NOE enhanced) spectrum and are reported in hertz. ^b Toluene- d_8 at -50°C , 100.25 MHz. ^c Cyclohexane- d_{12} at room temperature, 100.25 MHz.

ported.^{17c} Under the experimental conditions employed, only one signal (or two in the case of the scandium ethyl complex) for the alkyl ligand of each scandium complex in solution is observed (Table II).

Kinetic measurements were carried out at $-80 (\pm 1)^\circ\text{C}$ under conditions of ca. 0.1 M scandium complex and 1–1.5 M ethylene in toluene- d_8 (see Experimental Section for details of sample preparation and spectra acquisition). Figure 1 shows a partial

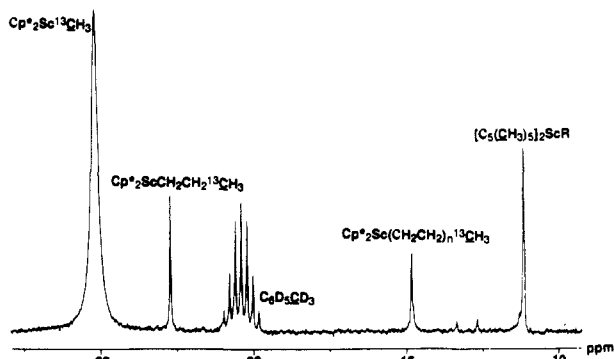


Figure 1. Partial ^{13}C NMR spectrum of a polymerization run of $\text{Cp}^*_2\text{Sc}^{13}\text{CH}_3$ and $\text{CH}_2=\text{CH}_2$ (toluene- d_8 , -80°C).

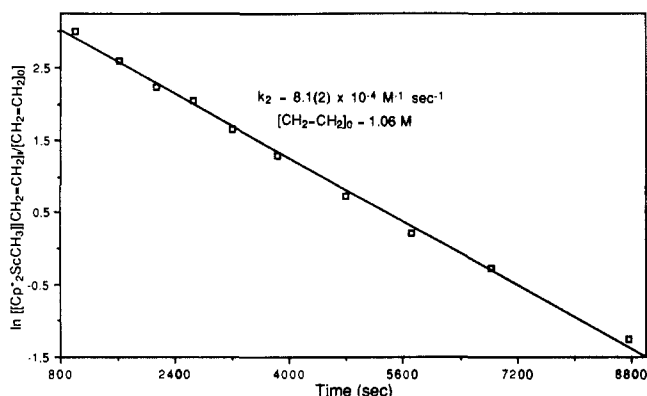


Figure 2. Representative kinetics plot for the reaction of $\text{Cp}^*_2\text{Sc}^{13}\text{CH}_3$ and $\text{CH}_2=\text{CH}_2$ (toluene- d_8 , -80°C).

spectrum acquired during a kinetics run of $\text{Cp}^*_2\text{Sc}^{13}\text{CH}_3$ and C_2H_4 . The resonance for the methyl ligand (δ 25.4) is considerably broadened (fwhh = 29 Hz, -80°C) due to its proximity to the quadrupolar scandium nucleus ($I = 7/2$, 100% abundance, -0.22 barn 22). The sharp singlets at δ 22.8 and 14.7 are assigned to the terminal carbons of the propyl and pentyl complexes, respectively (the signal for the terminal carbon of longer chain alkyl complexes cannot be resolved from that of the pentyl complex; see Table II). The methyl groups on the Cp^* rings for the scandium alkyl complexes in solution are not resolved but rather appear as a single resonance at δ 11.5. The septet at δ 20.4 is due to the solvent ($\text{C}_6\text{D}_5\text{CD}_3$). Resonances due to unreacted ethylene, ferrocene (added as an internal standard), and the other solvent signals are not shown in this partial spectrum.

From each spectrum, the relative integrations of the two starting materials, $\text{Cp}^*_2\text{Sc}^{13}\text{CH}_3$ and C_2H_4 , were determined. Since ethylene is reacting not only with $\text{Cp}^*_2\text{Sc}^{13}\text{CH}_3$ but also with each of the products, its concentration does not remain approximately constant, even when added initially in large excess. Thus, standard techniques for obtaining second-order rate constants do not apply. 23 Data were therefore plotted as for pseudo-first-order kinetics with a correction ($[\text{C}_2\text{H}_4]_t/[\text{C}_2\text{H}_4]_0$) made at each data point to compensate for the steadily decreasing concentration of ethylene in solution. 24 A representative plot of the kinetics ($\ln \{[\text{ScR}][\text{C}_2\text{H}_4]_t/[\text{C}_2\text{H}_4]_0\}$ vs time) for the reaction of $\text{Cp}^*_2\text{Sc}^{13}\text{CH}_3$ and ethylene is shown in Figure 2. From the slope an observed rate constant, k_{obs} , was obtained. The second-order rate constant, k_2 , may then be calculated: $k_2 = k_{\text{obs}}/[\text{C}_2\text{H}_4]_0$, where $[\text{C}_2\text{H}_4]_0$

(22) Becker, E. D. *High Resolution NMR*; Academic: New York, 1980; p 282.

(23) Moore, J. W.; Pearson, R. G. *Kinetics and Mechanism*; Wiley-Interscience: New York, 1981; Chapter 8.

(24) The correction factor applied to each data point is $[\text{C}_2\text{H}_4]_t/[\text{C}_2\text{H}_4]_0$, which accounts for the continuous disappearance of ethylene. For example, when the ethylene supply is 75% depleted, the rate of disappearance of Cp^*_2ScR is one-quarter of the initial rate or the rate if the ethylene concentration could be held constant. Therefore the correction factor of 0.25 is included to yield an apparent pseudo-first-order reaction.

Table III. Second-Order Rate Constants (k_2) for the Reaction of Ethylene with Cp^*_2ScR Complexes a

R	$k_2(-80^\circ\text{C})$, $\text{M}^{-1}\text{s}^{-1}$
$^{13}\text{CH}_3$	$8.1(2) \times 10^{-4}$
$^{13}\text{CH}_2^{13}\text{CH}_3$	$4.4(2) \times 10^{-4}$
$\text{CH}_2\text{CH}_2^{13}\text{CH}_3$	$6.1(2) \times 10^{-3}$

a Rate constants were measured by a continuous accumulation stacking routine with sufficient duration allowed between pulses to enable quantitative information to be derived from relative integration of resonances of interest.

Table IV. Second-Order Rate Constants (k_2) for the Reaction of $\text{Cp}^*_2\text{ScCH}_3$ and 2-Butyne a

T, K	$k_2 \times 10^4$, $\text{M}^{-1}\text{s}^{-1}$	T, K	$k_2 \times 10^4$, $\text{M}^{-1}\text{s}^{-1}$
245	1.28 (3)	260	4.31 (8)
250	2.34 (4)	265	6.38 (14)

a Butyne concentrations were measured by use of an internal standard (Cp_2Fe) of known concentration.

Table V. Second-Order Rate Constants (k_2) for the Reaction of $\text{Cp}^*_2\text{ScCH}_3$ and Unsymmetrical Alkynes ($\text{RC}\equiv\text{CR}'$) a

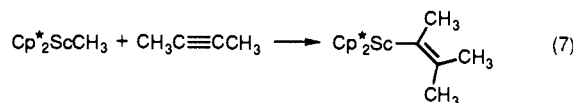
R	R'	$k_A(255\text{K}) \times 10^5$, $\text{M}^{-1}\text{s}^{-1}$	$k_B(255\text{K}) \times 10^5$, $\text{M}^{-1}\text{s}^{-1}$	A:B
CH_3	CH_3	15 (1)	15 (1)	50:50
CH_3	CH_2CH_3	21 (1)	10 (1)	68:32
CH_3	C_6H_5	1.4 (1)	0.91 (1)	61:39
CH_3	$\text{CH}(\text{CH}_3)_2$	0.16 (1)		100:0

a Products A and B are as shown in eq 10 (see text). The rate constants, k_A and k_B , are for the formation of A and B, respectively.

represents the initial ethylene concentration.

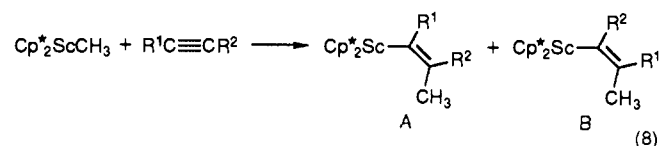
Rate constants were obtained analogously for $\text{Cp}^*_2\text{Sc}^{13}\text{CH}_2^{13}\text{CH}_3$ and $\text{Cp}^*_2\text{ScCH}_2\text{CH}_2^{13}\text{CH}_3$ (Table III). Attempts to obtain rate constants at different temperatures were unsuccessful; lower temperatures resulted in viscosity and solubility problems, and reaction rates too fast for NMR measurement were observed at higher temperatures.

Reaction of $\text{Cp}^*_2\text{ScCH}_3$ With Internal Alkynes. Previous studies 17b have shown that $\text{Cp}^*_2\text{ScCH}_3$ reacts with 2-butyne to form the product of a single insertion, $\text{Cp}^*_2\text{ScC}(\text{CH}_3)=\text{C}(\text{CH}_3)_2$ (eq 7). No further reaction is observed (>35 equiv of butyne,



1 day at 80°C). The kinetics for the formation of $\text{Cp}^*_2\text{Sc}-\text{C}(\text{CH}_3)=\text{C}(\text{CH}_3)_2$ can be followed conveniently by ^1H NMR (toluene- d_8) and serve as a model for a single insertion step in the polymerization of ethylene discussed previously. Pseudo-first-order kinetics were obtained over at least 2 half-lives. Second-order rate constants were obtained over the temperature range 245–265 K (Table IV). Activation parameters, derived from an Eyring plot, are as follows: $\Delta G^\ddagger(265\text{K}) = 18.95$ (1) kcal/mol $^{-1}$, $\Delta S^\ddagger = -36$ (2) eu, $\Delta H^\ddagger = 9.7$ (3) kcal/mol.

Alkyne insertion into the $\text{Sc}-\text{CH}_3$ bond occurs for a variety of different internal alkynes. With unsymmetrical alkynes two products can arise, depending on the orientation of the alkyne (eq 8). Isomeric assignment of A and B were made by comparison with authentic samples (see Experimental Section).



The kinetics for the formation of A and B were monitored as described above for the reaction of $\text{Cp}^*_2\text{ScCH}_3$ with 2-butyne. The rate constant obtained from the pseudo-first-order plots, k_{obs} , in these experiments is a sum of the rate constants for the for-

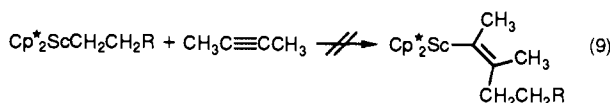
Table VI. Observed Rate Constants (k_{obs}) for β -Hydrogen Elimination of $\text{Cp}^*_2\text{ScCH}_2\text{CH}_2\text{Ph}$ as a Function of 2-Butyne Concentration^a

[2-butyne], M	$k_{\text{obs}} \times 10^4, \text{s}^{-1}$	[2-butyne], M	$k_{\text{obs}} \times 10^4, \text{s}^{-1}$
0.98	3.16 (6)	2.87	3.30 (5)
1.17	2.97 (11)	3.35	2.98 (2)

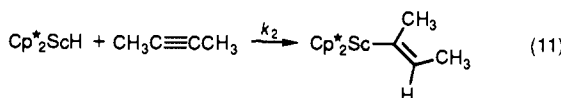
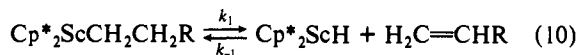
^aRate constants were measured at 285 K. Butyne concentrations were measured by using an internal standard [$(\eta^5\text{-C}_5\text{H}_5)_2\text{Fe}$] of known concentration.

mation of A and B: $k_{\text{obs}} = k_A + k_B$; the ratio of products obtained yields k_A/k_B (Table V).²⁵

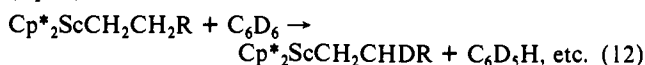
β -Hydrogen Elimination of Permethylscandocene Alkyl Complexes. While investigating the stoichiometric reactions of permethylscandocene alkyl complexes with internal alkynes, it was observed that no insertion took place for scandium alkyl complexes containing β -hydrogens (eq 9). Rather, the products of this



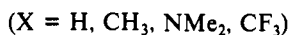
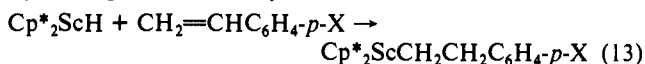
reaction were *cis*- $\text{Cp}^*_2\text{Sc}(\text{CH}_3)\text{C}=\text{CH}(\text{CH}_3)$ and free olefin, $\text{CH}_2=\text{CHR}$. These products are consistent with β -hydrogen elimination to form free olefin and Cp^*_2ScH ; the latter is readily trapped by the alkyne in solution (eq 10 and 11). (*E*-)



$\text{Cp}^*_2\text{Sc}(\text{CH}_3)\text{C}=\text{CH}(\text{CH}_3)$ has been prepared independently (vide infra). Further evidence that reversible β -hydrogen elimination occurs in solution is garnered from the observation of deuterium incorporation in the β position when the scandium alkyl complex is dissolved in benzene-*d*₆.²⁶ Deuterium incorporation likely proceeds via the reversible reaction of Cp^*_2ScH with C_6D_6 ^{17c} (eq 12).

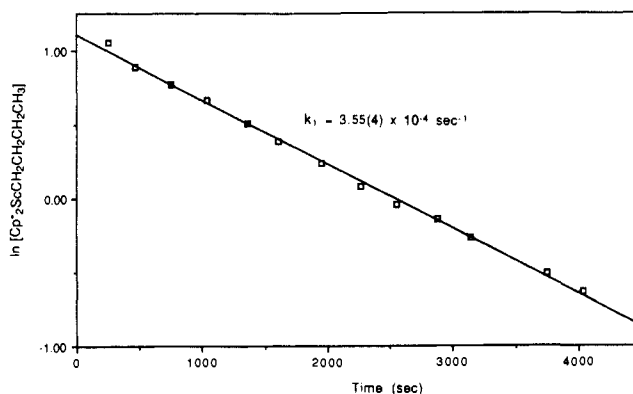


A series of permethylscandocene alkyl complexes have been prepared in order to probe the steric and electronic effects of the β -hydrogen elimination reaction. The syntheses of the ethyl and propyl complexes have been previously reported.^{17c} The phenethyl derivatives are prepared analogously by using the appropriate styrene (eq 13). Yellow crystalline materials are obtained in each



case, although isolated yields (40–65%) are only moderate owing to the very high solubility of these compounds. ¹H and ¹³C NMR spectra are unexceptional, being characterized by AA'BB' multiplets for the $\text{ScCH}_2\text{CH}_2\text{Ph}$ protons and signals for the β -carbons appearing at ca. δ 36 ($J_{\text{CH}} = 118\text{--}122$ Hz) (Table II). Very soluble $\text{Cp}^*_2\text{ScCH}_2\text{CH}_2\text{CH}_2\text{CH}_3$ is prepared by a method analogous to that described above using a stoichiometric amount of the 1-butene.

β -Hydrogen Elimination Rate Kinetic Measurements. The observed rate constants for the reaction of $\text{Cp}^*_2\text{ScCH}_2\text{CH}_2\text{Ph}$ with 2-butyne (toluene-*d*₈, ¹H NMR, 280 K) were found to be independent of butyne concentration over the range 0.98–3.35 M

**Figure 3.** Kinetics plot of the reaction of $\text{Cp}^*_2\text{ScCH}_2\text{CH}_2\text{CH}_2\text{CH}_3$ with 2-butyne (toluene-*d*₈, 2 °C, 1.11 M 2-butyne).**Table VII.** Kinetic Data for β -Hydrogen Elimination of Cp^*_2ScR Complexes^a

R	$k_1 \times 10^4, \text{s}^{-1}$	$\Delta G^\ddagger, \text{kcal/mol}$
CH_2CH_3	0.94 (3)	21.51 (8)
$\text{CH}_2\text{CH}_2\text{CH}_3$	6.3 (1)	20.45 (7)
$\text{CH}_2\text{CH}_2\text{SiMe}_3$	0.02 (1) ^b	24.9 (2)
$\text{CH}_2\text{CH}_2\text{CH}_2\text{CH}_3$	3.55 (4)	20.77 (7)
$\text{CH}_2\text{CH}_2\text{Ph}$	1.67 (3)	21.19 (8)
$\text{CH}_2\text{CH}_2\text{Ph-}p\text{-NMe}_2$	42 (1) ^c	19.40 (8)
$\text{CH}_2\text{CH}_2\text{Ph-}p\text{-CF}_3$	0.11 (1) ^d	22.71 (9)
$\text{CH}_2\text{CH}_2\text{Ph-}p\text{-CH}_3$	3.26 (6)	20.82 (8)

^aRate constants and free energies of activation listed are for 280 K. Errors in ΔG^\ddagger represent one standard deviation estimated from the uncertainties in k_1 (280) and the temperature. ^bExtrapolated from k_1 and ΔG^\ddagger measured at 298 K assuming $\Delta S^\ddagger = -11$ eu. ^cExtrapolated from k_1 and ΔG^\ddagger measured at 265 K assuming $\Delta S^\ddagger = -11$ eu. ^dExtrapolated from k_1 and ΔG^\ddagger measured at 295 K assuming $\Delta S^\ddagger = -11$ eu.

Table VIII. Rate Constants for β -Hydrogen Elimination of Cp^*_2ScR Complexes

R	T, K	k_1, s^{-1}
CH_2CH_3	275	$5.29 (7) \times 10^{-5}$
	280	$9.4 (3) \times 10^{-5}$
	284	$2.18 (3) \times 10^{-5}$
	290	$3.98 (10) \times 10^{-4}$
	296	$6.93 (16) \times 10^{-4}$
$\text{CH}_2\text{CH}_2\text{CH}_3$	265	$7.9 (2) \times 10^{-5}$
	270	$1.72 (4) \times 10^{-4}$
	275	$3.01 (2) \times 10^{-4}$
$\text{CH}_2\text{CH}_2\text{CH}_2\text{CH}_3$	270	$1.21 (2) \times 10^{-4}$
	275	$1.99 (2) \times 10^{-4}$
	280	$3.55 (4) \times 10^{-4}$
	285	$7.6 (3) \times 10^{-4}$
$\text{CH}_2\text{CH}_2\text{SiMe}_3$	298	$\approx 5.3 (8) \times 10^{-6}$
	270	$5.14 (9) \times 10^{-5}$
$\text{CH}_2\text{CH}_2\text{Ph}$	275	$6.5 (2) \times 10^{-5}$
	280	$1.67 (3) \times 10^{-4}$
	285	$3.16 (6) \times 10^{-4}$
	290	$5.23 (10) \times 10^{-4}$
	270	$1.00 (4) \times 10^{-4}$
$\text{CH}_2\text{CH}_2\text{Ph-}p\text{-CH}_3$	280	$3.26 (6) \times 10^{-4}$
	290	$1.04 (2) \times 10^{-3}$
	265	$3.74 (5) \times 10^{-6}$
$\text{CH}_2\text{CH}_2\text{Ph-}p\text{-CF}_3$	295	$1.32 (4) \times 10^{-4}$
	300	$2.26 (4) \times 10^{-4}$
	305	$5.66 (16) \times 10^{-4}$

(Table VI). This favorable situation allows direct measurement of the rate constant of interest, $k_1 = k_{\text{obs}}$, since the reverse process k_{-1} does not effectively compete with 2-butyne trapping (k_2).

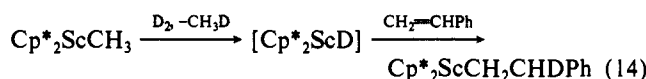
A representative kinetics plot for the reaction of $\text{Cp}^*_2\text{ScCH}_2\text{CH}_2\text{CH}_2\text{CH}_3$ with 2-butyne is shown in Figure 3. First-order rate constants (k_1) and free energies of activation

(25) Reference 20, pp 22–25.

(26) Deuterium incorporation in the β position of $\text{Cp}^*_2\text{ScCH}_2\text{CH}_2\text{CH}_2\text{CH}_3$ was observed in the ¹³C{¹H} NMR spectrum (C_6D_6 , 25 °C). A 1:1:1 triplet at δ 34.0 ($J_{\text{CD}} = 18$ Hz) (isotopically shifted from the signal for the perproton complex at δ 34.5) is assigned to the β -carbon with one bound deuterium, $\text{Cp}^*_2\text{ScCH}_2\text{CHDCH}_2\text{CH}_3$.

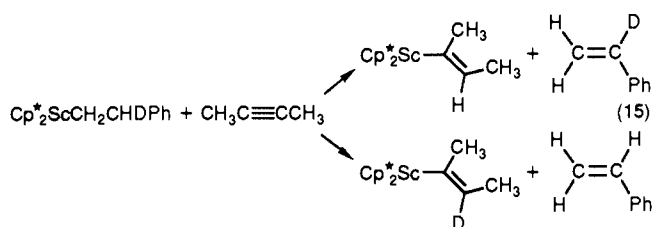
(ΔG^\ddagger) are listed for each complex in Table VII. A complete listing of all rate constants measured is given in Table VIII. Activation parameters for the decomposition of $\text{Cp}^*_2\text{ScCH}_2\text{CH}_2\text{C}_6\text{H}_5$ and $\text{Cp}^*_2\text{ScCH}_2\text{CH}_2\text{C}_6\text{H}_4\text{-}p\text{-CH}_3$, derived from Eyring plots are as follows: $\Delta G^\ddagger(280\text{ K}) = 21.19$ (8) $\text{kcal}\cdot\text{mol}^{-1}$, $\Delta S^\ddagger = -11$ (2) eu, $\Delta H^\ddagger = 17.98$ (44) $\text{kcal}\cdot\text{mol}^{-1}$; $\Delta G^\ddagger(280\text{ K}) = 20.82$ (8) $\text{kcal}\cdot\text{mol}^{-1}$, $\Delta S^\ddagger = -10$ (1) eu, $\Delta H^\ddagger = 18.04$ (28) $\text{kcal}\cdot\text{mol}^{-1}$, respectively.

Deuterium Kinetic Isotope Effect on the β -Hydrogen Elimination. Kinetic deuterium isotope effects on the β -hydrogen elimination rate were measured for $\text{Cp}^*_2\text{ScCH}_2\text{CHDC}_6\text{H}_5$, prepared by adding 1 equiv of styrene to a petroleum ether solution of Cp^*_2ScD (eq 14). High-field ^2H and ^1H NMR showed con-



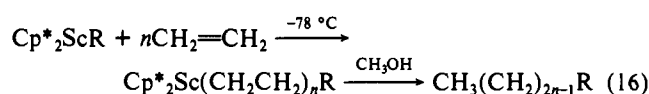
clusively that the deuterium is located solely in the β position and that incorporation is greater than 95%.

Treatment of $\text{Cp}^*_2\text{ScCH}_2\text{CHDC}_6\text{H}_5$ with excess 2-butyne in benzene- d_6 at room temperature affords a mixture of products (eq 15). The ratio of $\text{CH}_2=\text{CHC}_6\text{H}_5$ to $\text{CH}_2=\text{CDC}_6\text{H}_5$ was



determined by cutting and weighing the peaks corresponding to the hydrogen cis to the phenyl group from the ^1H NMR spectrum (400 MHz). A deuterium kinetic isotope effect ($k_{\text{H}}/k_{\text{D}}$) of 2.0 (3) was obtained from the ratio of styrene- d_0 to styrene- d_1 .

Studies of Ethylene Oligomers. Molecular weight distributions for oligomers obtained from reaction of Cp^*_2ScR with ethylene have been examined by gas chromatography. Samples were typically prepared by treating the appropriate scandium alkyl complex with 40 equiv of ethylene (accurately measured) at -78°C in toluene or petroleum ether. Excess ethylene was subsequently removed and measured with a Toepler pump, and the Sc-alkyl bonds were cleaved with excess methanol, yielding straight-chain alkane products (eq 16). The scandium byproducts



were hydrolyzed to the oxide with excess H_2O , and the organics were extracted for GC analysis by comparison to authentic alkane standards. Alkanes of fewer than 13 carbons were obscured by solvent- and pentamethylcyclopentadiene-associated peaks. The range of observable products was limited to alkanes of fewer than 50 carbons by the maximum operating temperature of the GC column.

As shown in Figure 4, reaction of $\text{Cp}^*_2\text{ScCH}_2\text{CH}_2\text{CH}_3$ with ethylene produces only alkanes with odd numbers of carbons. In Figure 5 the quantitated data from a series of reactions are plotted along with Poisson distributions (vide infra) based on the number of equivalents of ethylene consumed (as determined by Toepler pump measurements). At conversions slightly higher than those shown, ca. 10 equiv of ethylene consumed, the heavier alkyls begin to precipitate from the reaction mixture, and significant deviations from Poisson statistics are observed.

The differences observed for the oligomerization of identical amounts of ethylene, when initiated with either $\text{Cp}^*_2\text{ScCH}_2\text{CH}_2\text{CH}_3$ or $\text{Cp}^*_2\text{ScCH}_3$, are illustrated in Figure 6. As in the case of oligomerization initiated by $\text{Cp}^*_2\text{ScCH}_2\text{CH}_2\text{CH}_3$, the reaction of ethylene with $\text{Cp}^*_2\text{ScCH}_3$ produces only alkanes with an odd number of carbons. Experiments initiated with $\text{Cp}^*_2\text{ScCH}_2\text{CH}_3$ resulted in precipitation of product after con-

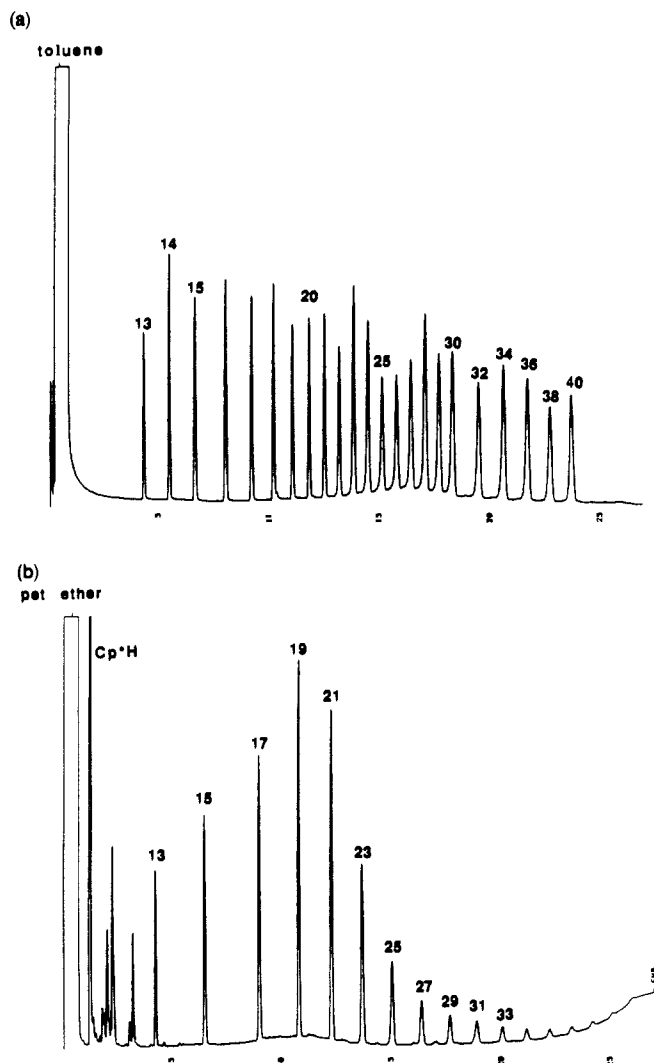


Figure 4. Sample chromatograms. (a) Standard sample prepared from commercial alkanes. Bold numbers indicate number of carbons in the eluting n -alkane. (b) Typical reaction mixture ($\text{Cp}^*_2\text{ScCH}_2\text{CH}_2\text{CH}_3$ + 7.8 equiv of ethylene, petroleum ether).

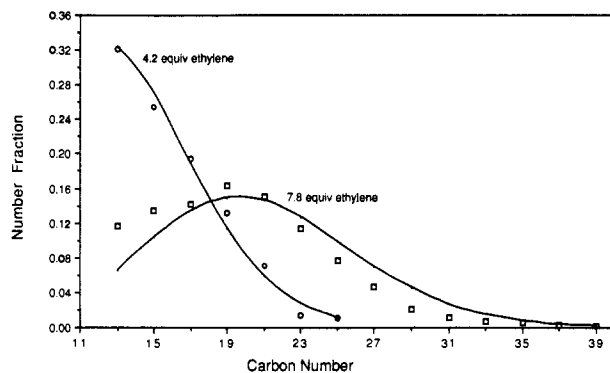


Figure 5. Oligoethylenes from $\text{Cp}^*_2\text{ScCH}_2\text{CH}_2\text{CH}_3$. O: solvent, toluene, 4.2 equiv of ethylene consumed. \square : solvent, petroleum ether, 7.8 equiv consumed. Solid lines indicate corresponding Poisson distributions (see text).

sumption of only 4 equiv of ethylene; the product distribution obtained after consumption of 2 equiv of ethylene is shown in Figure 7.

Discussion

The rates for ethylene insertion for Cp^*_2ScR vary with the nature of the alkyl group ($\text{R} = \text{CH}_3, \text{CH}_2\text{CH}_3, \text{CH}_2\text{CH}_2\text{CH}_3$) over a factor of approximately 15: $\text{Sc}-\text{CH}_2\text{CH}_2\text{CH}_3 > \text{Sc}-\text{CH}_3 > \text{Sc}-\text{CH}_2\text{CH}_3$ (Table III). The rate of ethylene insertion for

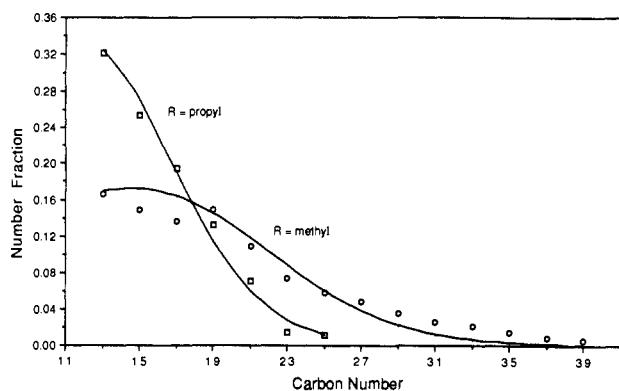


Figure 6. Oligoethylenes from Cp^*_2ScR . \square : R = propyl; solvent, toluene, 4.2 equiv of ethylene consumed. \circ : R = methyl; solvent, toluene, 4.3 equiv of ethylene consumed. Solid lines indicate model distributions (see text).

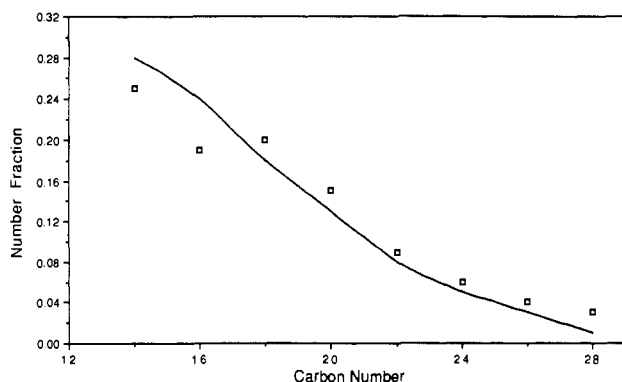
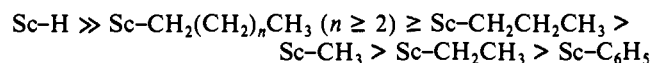


Figure 7. Oligoethylenes from $\text{Cp}^*_2\text{ScCH}_2\text{CH}_3$. Solvent, toluene, 2.0 equiv of ethylene consumed. Solid line indicates model distribution (see text).

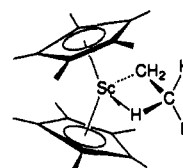
Cp^*_2ScH is too fast to measure by the methods used here; complete conversion to $\text{Cp}^*_2\text{ScCH}_2\text{CH}_3$ occurs before the first spectrum may be recorded (40 equiv of ethylene, toluene- d_8 , quickly thawed to -80°C in the NMR probe); a very conservative lower limit of ca. $10^{-2}\text{ s}^{-1}\text{M}^{-1}$ for the rate constant for the reaction of Cp^*_2ScH with C_2H_4 is estimated. We also note that ethylene insertion into the scandium-phenyl bond for $\text{Cp}^*_2\text{ScC}_6\text{H}_5$ is much slower than insertion into scandium-alkyl bonds.²⁷ Moreover, the satisfactory fits to a Poisson distribution for the molecular weights of the oligomers initiated with $\text{Cp}^*_2\text{ScCH}_2\text{CH}_2\text{CH}_3$, calculated by using a propagation rate constant equal to that for insertion of ethylene into the $\text{Sc}-\text{CH}_2\text{CH}_2\text{CH}_3$ bond (vide infra), suggests that for alkyls larger than propyl, $k_2 \geq 6 \times 10^{-3}\text{ s}^{-1}\text{M}^{-1}$. Thus, the order of decreasing rates of ethylene insertion is



The faster rate for insertion for the hydride derivative was expected and almost certainly is due to the greater overlap, hence better bonding in the transition state for H (nondirectional $1s$ orbital) vs alkyl (more directional sp^3 hybrid orbital). On the other hand, the greater insertion rate observed for scandium propyl relative to the scandium methyl is likely due to ground-state differences. Since considerable scandium-carbon bond breaking is expected in the transition state for a concerted process like ethylene insertion, the strength of the metal-carbon bond directly affects the magnitude of the activation barrier: a stronger metal-carbon bond will result in a higher activation barrier (slower insertion rate). Equilibrium measurements indicate that the relative ordering of $\text{Sc}-\text{R}$ bond dissociation energies (BDEs) will mirror that for the corresponding $\text{H}-\text{R}$ BDEs;^{17d,28} hence, BDE-

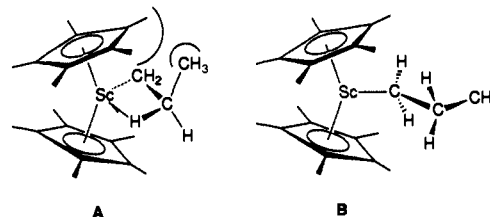
$(\text{Sc}-\text{CH}_3) - \text{BDE}(\text{Sc}-\text{CH}_2\text{CH}_2\text{CH}_3) \geq \text{ca. } 6 \text{ kcal}\cdot\text{mol}^{-1}$. These conclusions are also supported by the results from reaction calorimetry reported by Marks and co-workers for hydride, alkyl, and aryl derivatives of permethylthorocene, $\text{Cp}^*_2\text{ThR}_2$.²⁹ Although experimental difficulties precluded measuring the activation parameters, the factor of only 15 favoring insertion into $\text{Sc}-\text{CH}_2\text{CH}_2\text{CH}_3$ [much less than the $>10^6$ ratio expected if $\Delta(\Delta H^\ddagger) \approx \Delta(\text{BDE})$] probably also reflects the larger steric barrier for the propyl group. Bond strength considerations undoubtedly are also responsible for the relative inactivity of the scandium phenyl complex toward ethylene.

The observation that the scandium ethyl complex is slowest to insert ethylene cannot be reasonably rationalized by these types of metal-carbon bond strength considerations or by transition-state differences. An examination of its structure provides insight into the decreased reactivity toward ethylene relative to the other alkyl complexes studied. Evidence points to a β -agostic interaction in the ground state, as shown:



Although ^{13}C and ^1H NMR data are not diagnostic of a static or rapidly fluxional agostic structure,³⁰ IR spectroscopy reveals low-energy C-H bands indicative of the agostic interaction. Moreover, the crystal structure determination for $\text{Cp}^*_2\text{ScCH}_2\text{CH}_3$ indicated similar $\text{Sc}-\text{C}_\alpha$ and $\text{Sc}-\text{C}_\beta$ bond lengths; however, disorder in the $\eta^5-\text{C}_5\text{Me}_5$ rings precluded accurate resolution of the ethyl ligand.³¹

A similar β -agostic interaction for the scandium propyl complex, although electronically favorable, is sterically unfavorable. Donation of electron density from one of the β -C-H bonds into an empty orbital on scandium requires that the bond be held in the equatorial plane of the "bent sandwich", and as such, the methyl group on the β -carbon is directed toward one of the $\eta^5-\text{C}_5\text{Me}_5$ rings (as shown in A).



These adverse steric interactions for the propyl complex are apparently sufficiently destabilizing that the conventional structure B is favored, as indicated by the IR spectrum of the scandium propyl complex (no low-energy C-H bands signifying structure A).³²

(28) (a) Bryndza, H. E.; Fong, L. K.; Paciello, R. A.; Tam, W.; Bercaw, J. E. *J. Am. Chem. Soc.* **1987**, *109*, 1444. (b) Bryndza, H. E.; Domaille, P. J.; Fong, L. K.; Paciello, R. A.; Tam, W.; Bercaw, J. E. *Polyhedron* **1988**, *7*, 1441-1452.

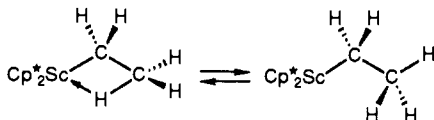
(29) Bruno, J. W.; Marks, T. J.; Morss, L. R. *J. Am. Chem. Soc.* **1983**, *105*, 6824-6832.

(30) (a) Brookhart, M.; Green, M. L. H. *J. Organomet. Chem.* **1983**, *250*, 395. (b) Lamanna, W.; Brookhart, M. *J. Am. Chem. Soc.* **1981**, *103*, 989. (c) Brookhart, M.; Lamanna, W.; Humphrey, M. B. *J. Am. Chem. Soc.* **1982**, *104*, 2117. (d) Brookhart, M.; Lamanna, W.; Pinhas, A. R. *Organometallics* **1983**, *2*, 638. (e) Dawoodi, Z.; Green, M. L. H.; Mtetwa, V. S. B.; Prout, K. *J. Chem. Soc., Chem. Commun.* **1982**, 802. (f) Dawoodi, Z.; Green, M. L. H.; Mtetwa, V. S. B.; Prout, K.; Schultz, A. J.; Williams, J. M.; Koetzle, T. F. *J. Chem. Soc., Dalton Trans.*, in press. (g) Berry, A.; Dawoodi, Z.; Derome, A. E.; Dickinson, J. M.; Downs, A. J.; Green, J. C.; Green, M. L. H.; Hare, P. M.; Payne, M. P.; Rankin, D. W. H.; Robertson, H. E. *J. Chem. Soc., Chem. Commun.*, in press.

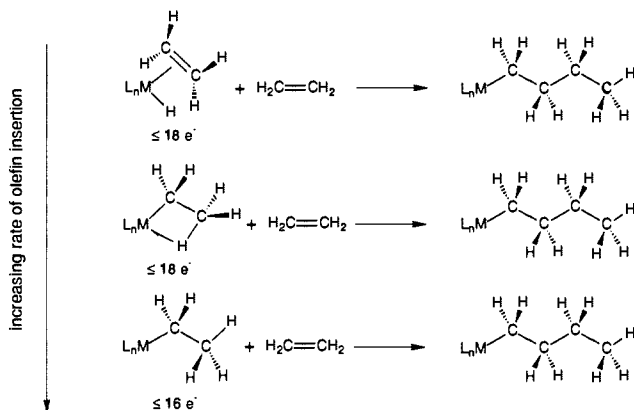
(31) Okamoto, J. K.; St. Clair, M. A.; Schaefer, W. P.; Bercaw, J. E., unpublished results.

(27) There is a slow reaction between Cp^*_2ScPh and C_2H_4 at room temperature; however, the rate of this reaction was not quantified.

This agostic interaction for the scandium ethyl complex results in a ground-state stabilization relative to that of the conventional $14e^-$ alkyl complexes [i.e., $Cp^*_2ScCH_2(CH_2)_nCH_3$, $n \geq 1$]. Presumably, this interaction first must be broken, increasing the barrier toward ethylene insertion relative to the other alkyl complexes.



Schmidt and Brookhart³³ have proposed a correlation between a structure with an agostic β -hydrogen interaction (vs olefin-hydride) and that compounds' propensity for undergoing olefin insertion into the incipient metal-alkyl bond. A series of complexes, $[CpCo(L)(CH_2CH_2)H]^+$, where L is a phosphine or phosphite ligand, were shown to adopt agostic structures and also to be active polymerization catalysts. 1H NMR studies showed that the products of ethylene insertion reaction likewise contain agostic structures, and that insertion of ethylene into the $Co-CH_2CH_3$ bond is slower than subsequent insertions. Our results appear to indicate that, all other factors equal, an alkyl complex that is coordinatively unsaturated will be more reactive toward alkyl migration than one for which there is an agostic interaction, which Brookhart et al. have in turn shown to be more reactive than a traditional olefin hydride.



The distributions of products resulting from the oligomerization of ethylene by permethylscandocene alkyls have been examined at low levels of ethylene consumption. Under the conditions examined, these complexes qualify as truly "living" catalysts for ethylene oligomerization (one for which chain propagation occurs at the same rate, regardless of chain length, and without competition from termination or chain-transfer pathways). The lack of chain transfer is also convincingly addressed by initiating oligomerization with an alkyl containing an odd number of carbons, e.g., $Cp^*_2ScCH_2CH_2CH_3$ and $Cp^*_2ScCH_3$. The observation that only odd carbon number chains are obtained (Figure 4) requires no chain transfer, since β -H elimination would yield Cp^*_2ScH ,

(32) A β C-H to Sc agostic interaction has also been observed in (*E*)- $Cp^*_2Sc(CH_3)C=CH(CH_3)$, one that involves the vinylic C-H bond. Due to the extreme solubility of this compound in inert solvents such as toluene and pentane, only samples of modest purity ($\leq 90\%$) have been isolated. Despite this limitation, spectral analysis of the isolated material is revealing. The 1H NMR chemical shift of the vinyl proton is, at δ 3.78, approximately 1.4 ppm upfield of the β -vinyl protons in the related compound (*E*)- $Cp^*_2ScCH=CH(CH_3)$, which does not appear to have an agostic C-H to Sc interaction.^{17c} The IR spectrum of (*E*)- $Cp^*_2Sc(CH_3)C=CH(CH_3)$ shows a low-energy C-H stretch at 2618 cm^{-1} . This band is not present in the spectrum of (*E*)- $Cp^*_2Sc(CH_3)C=CD(CH_3)$, having been replaced by a new band at 1960 cm^{-1} (calculated, 1911 cm^{-1}). A band at 1314 cm^{-1} , tentatively assigned to an out-of-plane C-H bend in the perprotio compound, shifts to 948 cm^{-1} (calculated, 959 cm^{-1}) upon deuteration at the vinylic position.

(33) (a) Schmidt, G. F.; Brookhart, M. *J. Am. Chem. Soc.* **1985**, *107*, 1443. (b) Brookhart, M.; Schmidt, G. F.; Lincoln, D. M.; Rivers, D. Olefin Insertion Reactions: The Mechanism of Co(III) Catalyzed Polymerization. In *Transition Metal Catalyzed Polymerization: Ziegler-Natta and Metathesis Polymerization*; Quirk, R. P., Ed.; Cambridge Press: New York, 1988.

which would subsequently undergo insertion to form $Cp^*_2ScCH_2CH_3$, etc., leading to an even carbon numbered chain. In contrast, at -40°C $Cp^*_2ScCH_2CH_2CH_3$ produces predominantly alkanes with an even number of carbons, indicating that chain transfer is a major pathway at higher temperatures.

If the additional mechanistic criterion is met that the initiation step is faster than, or at least as fast as, the propagation step, the distribution of products is governed by the Poisson distribution function and may be described as "monodisperse".³⁴ Because our GC analysis is necessarily limited to alkanes with fewer than 13 and greater than 50 carbons, polydispersity indexes are not particularly informative. We therefore chose to demonstrate monodispersity in these systems by direct comparison of the product distribution to a Poisson distribution based on the amount of ethylene consumed, assuming all scandium centers are functioning alike. As shown in Figure 5, agreement between the data and the Poisson distribution (both normalized to the observable product range) is good, when reaction is initiated with $Cp^*_2ScCH_2CH_2CH_3$ and at conversions of up to roughly 8 equiv of ethylene. The assumption that the rate of insertion into alkyls with three or more carbons is independent of chain length is thus substantiated (vide supra). If high molecular weight samples of polyethylene are prepared at -78°C , no oligomeric products are found in the supernatant upon workup, indicating that no chain transfer occurs even after long reaction times, regardless of the molecular weight distribution. Apparently, polymerization in this system ceases only when a long-chain alkyl complex precipitates from solution.

Theoretical product distributions for oligomerizations initiated by $Cp^*_2ScCH_3$ and $Cp^*_2ScCH_2CH_3$ cannot be calculated by using the Poisson function, since in these cases the first insertion is slower than subsequent ones (vide supra). Gold considered the effects of differing initiation and propagation rates in living systems over 30 years ago.³⁵ Qualitatively, the expectation is that as the initiation rate becomes slower, the distribution broadens and favors longer chain products, since molecules initiated early in the reaction consume a disproportionately large amount of monomer. By using the experimental rate constants to predict the oligomer distributions in these cases and performing simple iterative calculations on the concentrations of all species over small time intervals until a specified amount of ethylene is consumed, the molecular weight distributions for oligomers obtained from $Cp^*_2ScCH_3$ and $Cp^*_2ScCH_2CH_2CH_3$ may be predicted. Figure 6 (solid lines) shows the distribution calculated in this fashion for oligomerization beginning with $Cp^*_2ScCH_3$ alongside the distribution predicted by a Poisson function for an ethylene consumption of 4.2 equiv relative to scandium (i.e., with $Cp^*_2ScCH_2CH_2CH_3$ as initiating compound). Agreement between the experimental data and the predicted distributions is good in both the case of $Cp^*_2ScCH_3$ - and $Cp^*_2ScCH_2CH_2CH_3$ -initiated oligomerizations. This comparison vividly depicts the effect of the initiation rate on a living polymerization, even at very low monomer conversion. Similarly good agreement between observation and theory is obtained with oligomerization initiated by $Cp^*_2ScCH_2CH_3$, under conditions where the solution remains homogeneous, e.g., consumption of approximately 2 equiv of ethylene (Figure 7). The predominance of products corresponding to 10 or more insertions of monomer at such a low level of monomer conversion is a particularly dramatic illustration of the very slow initiation rate for $Cp^*_2ScCH_2CH_3$.

Our results with the scandium model system are in good agreement with product distributions of ethylene oligomerizations by $(\eta^5-C_3H_5)_2TiCl_2$ /chloroalkylaluminum systems at low temperatures.³⁶ It thus appears that the one-component scandium system is a good model for Ti/Al-based Ziegler catalysts, especially

(34) Szwarc, M.; Levy, M.; Milkovich, R. *J. Am. Chem. Soc.* **1956**, *78*, 2656.

(35) Gold, L. *J. Chem. Phys.* **1958**, *28*, 91.

(36) (a) Höcker, H.; Saeki, K. *Makromol. Chem.* **1971**, *148*, 107. (b) Cihlár, J.; Mejzlik, J.; Hamrik, O.; Hudec, P.; Majer, J. *Makromol. Chem.* **1980**, *181*, 2549. (c) Fink, G.; Zoller, W. *Makromol. Chem.* **1981**, *182*, 3265. (d) Fink, G.; Schnell, D. *Angew. Makromol. Chem.* **1982**, *105*, 15.

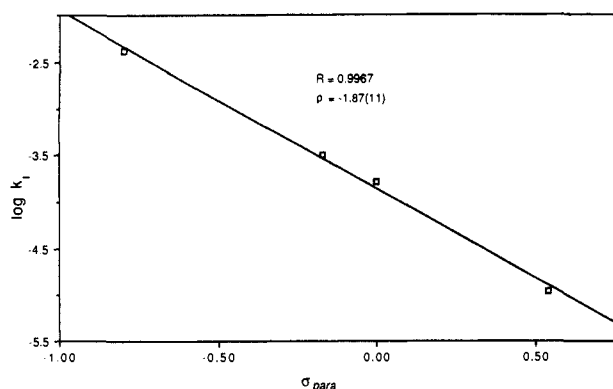
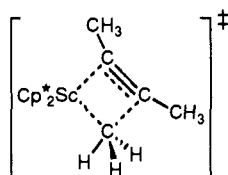


Figure 8. Hammett plot for the β -hydrogen elimination of permethylscandocene alkyl complexes.

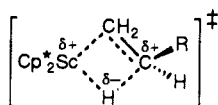
those with cyclopentadienyl ligands. These product distribution studies not only demonstrate the applicability of our kinetic studies to actual polymerizations performed with scandium catalysts, but also strengthen the argument that kinetic and mechanistic information obtained from these very simple systems is qualitatively applicable to the much more complicated classical Ziegler systems.

The stoichiometric reaction of $\text{Cp}^*_2\text{ScCH}_3$ with 2-butyne serves as a useful model for a single insertion step in the polymerization of ethylene. Second-order rate constants have been measured for this reaction over a range of temperatures allowing the determination of activation parameters. This reaction is characterized by a relatively small enthalpy of activation [$\Delta H^\ddagger = 9.7$ (3) $\text{kcal}\cdot\text{mol}^{-1}$] and a very large negative entropy of activation [$\Delta S^\ddagger = -36$ (2) eu]. These findings are consistent with a highly ordered four-centered transition state:



The importance of steric effects in these insertion reactions is illustrated by the reactions of $\text{Cp}^*_2\text{ScCH}_3$ with unsymmetrical alkynes. From the isomeric mixtures obtained with these reactions (Table V), it is apparent that formation of the isomer in which the bulky substituent is geminal to the scandium center is disfavored. Indeed, when the alkyne is 4-methyl-2-pentyne [$(\text{CH}_3)_2\text{CHC}\equiv\text{CCH}_3$], only one isomer, that with the isopropyl group directed away from the scandium, is formed. Although electronic effects may play some role in determining product distribution,³⁷ these appear to be smaller than the steric effects.

The β -hydrogen elimination rate for a series of permethylscandocene alkyl complexes has been measured by rapidly trapping Cp^*_2ScH as it forms with 2-butyne. From the data given in Table VII, it is clear that the β -hydrogen elimination rate is quite sensitive to the nature of the substituent(s) on the β -carbon. In order to focus solely on electronic effects, the β -hydrogen elimination rates for a series of para-substituted permethylscandocene phenethyl complexes were measured. Acceleration of the rate for electron-releasing para substituents (CH_3 or NMe_2) and deceleration for the electron-withdrawing para substituent (CF_3) indicates positive charge buildup in the transition state for β -hydrogen elimination.



(37) A transition state wherein there is development of partial positive charge on the β -carbon is indicated for the β -hydrogen elimination reaction (vide infra). If similar electronic effects are operative in the insertion reaction, orienting the alkyne such that the more electron-releasing substituent is trans to the scandium will be favored. Electronic effects on the insertion reaction were not, however, addressed in this study.

These data may be used to construct a Hammett plot ($\log k$ vs σ_p)³⁸ (Figure 8). The data give a good linear correlation with σ_p ($R = 0.9967$) with a slope (ρ) of -1.87 (11). The inferior linear correlation of $\log k$ vs σ_+ ($R = 0.9653$) suggests that direct resonance between the phenyl ring and the β -carbon is not maximized in the transition state. A likely explanation for this result is that as the hydrogen is transferred from the β -carbon to the scandium center, the phenyl group is twisted out of resonance with the incipient $\text{C}=\text{C}$ double bond to avoid steric interactions with a $\eta^5\text{-C}_5\text{Me}_5$ rings, as has been used to rationalize the correlation of the olefin insertion rate with σ_p for a series of para-substituted styrene hydride complexes of permethyl-niobocene.^{14b}

Substitution of a hydrogen at the β -carbon by an alkyl group (CH_3 or CH_2CH_3) or a phenyl group causes a modest increase in the β -hydrogen elimination rate. The relative order of rates, $R = \text{H} < \text{Ph} < \text{CH}_3$ for $\text{Cp}^*_2\text{ScCH}_2\text{CH}_2\text{R}$, may also be rationalized by this model of a transition state with a partial positive charge on the β -carbon. The alkyl groups are inductively electron releasing relative to hydrogen and thus stabilize the proposed transition state.³⁹ A phenyl group, while electron releasing by resonance, is inductively electron withdrawing. That the phenethyl complex undergoes β -hydrogen elimination more slowly than the propyl complex suggests that the electronic effect of the phenyl group is largely inductive in nature (vide supra).

The slightly faster decomposition rate of the propyl complex over that of the butyl complex further suggests that steric factors are operative in the transition state; the proper geometry for β -hydrogen elimination directs the substituent on the β -carbon atom toward a bulky $\eta^5\text{-C}_5\text{Me}_5$ ligand. Consequently, the butyl complex with a larger ethyl group on the β -carbon has a greater activation barrier and slower β -hydrogen elimination rate than the propyl complex. In accord, the analogous β -trimethylsilylethyl scandium complex undergoes very slow β -hydrogen elimination, and the scandium cyclopentylmethyl complex does not decompose via β -hydrogen elimination.⁴⁰ This reasoning, of course, implies that hydrogen transfer precedes $\text{Sc}-\text{C}_\alpha$ bond breaking. The results from this study are in contrast with those seen for pseudooctahedral cobalt complexes: alkylbis(dimethylglyoximate)cobalt(III) and related compounds,⁴¹ $[\text{Co}(\text{acac})\text{R}_2\text{L}_2]$ ($\text{L} = \text{PR}_3$),⁴² and alkylcobalamins⁴³ and the organocopper(I) compounds, L_nCuR ($\text{L} = \text{PMe}_3, \text{PPh}_3$).⁴⁴ For these complexes, bulky alkyl groups appear to accelerate the (effective) β -hydrogen elimination rate. On the other hand, Halpern has clearly shown that the β -elimination reactions for such complexes proceed via homolytic metal-carbon bond scission and subsequent H atom abstraction.⁴¹

The β -hydrogen elimination rates for $\text{Cp}^*_2\text{ScCH}_2\text{CH}_2\text{Ph}$ and $\text{Cp}^*_2\text{ScCH}_2\text{CH}_2\text{C}_6\text{H}_4\text{-}p\text{-CH}_3$ were measured over a range of temperatures, allowing activation parameters to be determined. These reactions are characterized by small, negative entropies of activation [-11 (2) and -10 (1) eu, respectively] consistent with the four-centered transition state proposed above. A similar value for ΔS^\ddagger has been obtained for β -hydrogen elimination for $[(\text{CH}_3)_2\text{CHCH}_2]_3\text{Al}$,⁴⁵ and it has been interpreted in terms of a reasonably tight, four-centered transition state with restricted rotation around the $\text{Al}-\text{C}$, $\text{C}-\text{C}$, and $\text{C}-\text{H}$ bonds. The kinetic isotope effect of 2.0 (3), measured for the β -hydrogen elimination

(38) Johnson, C. D. *The Hammett Equation*; Cambridge University Press: Cambridge, England, 1973; Chapter 1.

(39) Lowry, T. H.; Richardson, K. S. *Mechanism and Theory in Organic Chemistry*, 2nd ed.; Harper and Row, Publishers: New York, 1981; pp 130-145.

(40) β -Alkyl elimination predominates. Burger, B. J.; Bercaw, J. E., unpublished results.

(41) (a) Halpern, J.; Ng, F. T. T.; Rempel, G. L. *J. Am. Chem. Soc.* **1979**, *101*, 7124. (b) Tsou, T.-T.; Loots, M.; Halpern, J. *J. Am. Chem. Soc.* **1982**, *104*, 623. (c) Ng, F. T. T.; Rempel, G. L.; Halpern, J. *J. Am. Chem. Soc.* **1982**, *104*, 621. (d) Halpern, J. *Acc. Chem. Res.* **1982**, *15*, 238.

(42) Ikariya, T.; Yamamoto, A. *J. Organomet. Chem.* **1976**, *120*, 257.

(43) (a) Grate, J. H.; Schrauzer, G. N. *J. Am. Chem. Soc.* **1979**, *101*, 4601. (b) Schrauzer, G. N.; Grate, J. H. *J. Am. Chem. Soc.* **1981**, *103*, 541.

(44) (a) Miyashita, A.; Yamamoto, T.; Yamamoto, A. *Bull. Chem. Soc. Jpn.* **1977**, *50*, 1102. (b) *Ibid.* 1109.

(45) Egger, K. W. *J. Am. Chem. Soc.* **1969**, *91*, 2867.

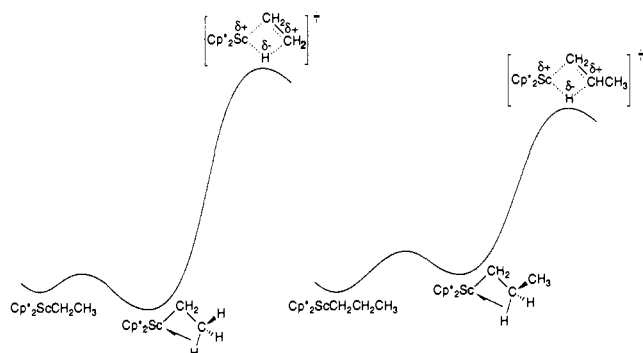


Figure 9. Partial free energy surfaces for β -hydrogen elimination of $\text{Cp}^*_2\text{ScCH}_2\text{CH}_3$ and $\text{Cp}^*_2\text{ScCH}_2\text{CH}_2\text{CH}_3$.

of $\text{Cp}^*_2\text{ScCH}_2\text{CH}_2\text{CH}_2\text{C}_6\text{H}_5$ ($Y = \text{H}, \text{D}$), also is in accord with the concerted nature of the β -hydrogen elimination with considerable C–H bond breaking in the transition state.⁴⁶ The transition state is thus pictured as four-centered with a partial positive charge on the β -carbon; hydrogen is transferred from the β -carbon to the electrophilic scandium center as H^- , an intuitively satisfying and altogether expected finding, given this same polarity found for the microscopic reverse, olefin insertion into M–H bonds, with less electrophilic transition-metal centers.^{14,47}

A curious result from this study is the relative ordering of the scandium ethyl and propyl complexes, in view of the β -agostic interaction in the ground-state structure of the ethyl complex (and no such interaction in the propyl complex). Since agostic interactions have been viewed as "arrested transition states" for hydride olefin insertion (and by microscopic reversibility, β -hydrogen elimination),^{30e} the slower rate of β -hydrogen elimination for the ethyl complex is at first surprising. The larger relative activation barrier for the ethyl complex undoubtedly arises from a ground-state stabilization for the ethyl derivative, attributable to the agostic interaction, and a transition-state stabilization for the propyl derivative, due to the stabilization of the positive charge by its β -methyl group. This reasoning can be used to construct qualitative partial free energy surfaces for the β -hydrogen elimination of $\text{Cp}^*_2\text{ScCH}_2\text{CH}_3$ and $\text{Cp}^*_2\text{ScCH}_2\text{CH}_2\text{CH}_3$, which are shown in Figure 9.⁴⁸

Conclusions

The rate of ethylene insertion into a series of permethylscandocene alkyls has been measured by ^{13}C NMR. The metal–carbon bond strength affects the insertion rate; a stronger bond results in a lower rate of insertion. Where sterically available, a ground-state stabilizing β -agostic interaction also serves to retard ethylene insertion. Results obtained for a single insertion of ethylene are directly applicable to the catalytic behavior of these one-component Ziegler systems. The set of rate constants measured for insertion into short-chain alkyl–scandium bonds may be used to calculate the molecular weight distributions of oligomeric products and thus for choosing conditions under which the oligomerization of ethylene can be shown to be "living". These results demonstrate the utility of systematic studies in rational Ziegler catalyst design.

The stoichiometric reaction of $\text{Cp}^*_2\text{ScCH}_3$ with internal alkynes has been examined as a model for a single insertion in the ethylene polymerization reaction. A highly ordered four-centered transition state is indicated. Due to the highly congested coordination sphere of the scandium center, steric effects play a dominant role in the transition state for this insertion reaction.

These permethylscandocene alkyl derivatives also provide a suitable model with which to probe β -hydrogen elimination. A

model for the transition state for β -hydrogen elimination has been developed. In accord with that proposed by others, the transition state is four-centered, with partial positive charge buildup at the β -carbon. The hydrogen is transferred to the scandium as H^- . The importance of steric effects in the transition state is underscored by the decreased rates of β -hydrogen elimination for the scandium cyclopentylmethyl and scandium β -trimethylsilylethyl complexes and suggest that hydrogen transfer precedes Sc– C_α bond cleavage.

Experimental Section

General Considerations. All manipulations were carried out with glovebox or high vacuum line techniques described previously.⁴⁹ Solvents were dried over LiAlH_4 or sodium benzophenone ketyl and stored over titanocene. Toluene- d_8 , benzene- d_6 , and cyclohexane- d_{12} were dried over activated 4-Å molecular sieves and stored over titanocene.

Argon, nitrogen, hydrogen, and deuterium were purified over MnO on vermiculite and activated molecule sieves. Ethylene (Matheson), propylene (Matheson), 1-butene (Matheson), ^{13}C – C_2H_4 (99% isotopic purity, MSD Isotopes), and ^{13}C –propylene (99% isotopic purity, MSD Isotopes) were purified by three cycles of freeze–pump–thaw at -196°C and then vacuum transferred at 25°C . ^{13}C –propylene was prepared by addition of acetaldehyde to ^{13}C –methylene triphenylphosphorane.

Styrene (Aldrich) and *p*-methylstyrene (Alfa) were used without further purification. *p*-(Trifluoromethyl)styrene was prepared by the literature method⁵⁰ except that the secondary alcohol, *p*- $\text{CF}_3\text{C}_6\text{H}_4\text{CH}(\text{OH})\text{CH}_3$ was formed by the reaction of CH_3MgBr and *p*- $\text{CF}_3\text{C}_6\text{H}_4\text{CHO}$ (Aldrich) in diethyl ether. *p*-(Dimethylamino)styrene was prepared by the reaction of *p*- $\text{NMe}_2\text{C}_6\text{H}_4\text{CHO}$ and CH_2PPh_3 in diethyl ether. *p*-(Trifluoromethyl)styrene and *p*-(dimethylamino)styrene were purified by vacuum distillation and characterized by ^1H NMR prior to use.

Alkynes were purchased and dried over activated molecular sieves prior to use: 2-butyne (Aldrich), phenylpropyne (Aldrich), 2-pentyne (Wiley), and 4-methyl-2-pentyne (Wiley). $(\eta^5\text{-C}_5\text{H}_5)_2\text{Fe}$, used as an internal standard for NMR tube kinetic experiments, was sublimed before use.

Alkanes used as standards for GC analysis—tridecane, tetradecane, pentadecane, hexadecane, heptadecane, octadecane, nonadecane, eicosane, heneicosane, docosane, tricosane, tetracosane, pentacosane, hexacosane, heptacosane, octacosane, nonacosane, triacontane, dotriacontane, tetratriacontane, hexatriacontane, octatriacontane, and tetracontane (Sigma)—were used as received.

NMR spectra were recorded on Varian EM-390 (^1H , 90-MHz), JEOL FX90Q (^1H , 89.56-MHz; ^{13}C , 22.50-MHz) and JEOL GX400Q (^1H , 399.78-MHz; ^{13}C , 100.38-MHz) spectrometers. Infrared spectra were recorded on a Beckman 4240 spectrometer and reported in cm^{-1} . All elemental analyses were conducted by L. Henling of the Caltech Analytical Laboratory. Oligomer analysis was performed on a Perkin-Elmer 8410 gas chromatograph and an Alltech RSL-150 macrobore column.

The syntheses of $\text{Cp}^*_2\text{ScCH}_3$, $\text{Cp}^*_2\text{Sc}^{13}\text{CH}_3$, $\text{Cp}^*_2\text{ScCH}_2\text{CH}_3$, $\text{Cp}^*_2\text{Sc}^{13}\text{CH}_2^{13}\text{CH}_3$, and $\text{Cp}^*_2\text{ScCH}_2\text{CH}_2\text{CH}_3$ have been reported previously.¹⁷

Ethylene Insertion Reactions: Sample Preparation. A typical sample was prepared in a glovebox by loading the Cp^*_2ScR complex (ca. 25 mg, 0.05 mmol) and 0.5 mL of toluene- d_8 [containing a known amount of $(\eta^5\text{-C}_5\text{H}_5)_2\text{Fe}$ as an internal standard] into a sealable NMR tube, which was then attached to a calibrated gas volume. The toluene solution was degassed at -78°C . Ethylene (ca. 0.5 mmol) was admitted to the gas volume and condensed into the NMR tube at -196°C . While the tube was kept at -196°C and open to the manifold, nitrogen (300 Torr) was admitted to the system. The tube was then sealed at -196°C . Fully immersed in a dry ice/diethyl ether bath (-100°C), the tube was sloshed to effect dissolution of the ethylene into the toluene solution. The solution was then refrozen at -196°C while the top half of the NMR tube was heated to thermally decompose any residual scandium complex on the walls of the tube.⁵¹ Warming in the dry ice/diethyl ether bath was

(49) *Organometallic Compounds*; Wayda, A. L., Darensbourg, M. Y., Eds.; ACS Symposium Series 357; American Chemical Society: Washington, DC, 1987.

(50) Baldwin, J. E.; Kapecki, J. A. *J. Am. Chem. Soc.* **1970**, *92*, 4869–4873.

(51) Only the lower portion (ca. 25%) of the NMR tube is cooled with the variable-temperature apparatus in the NMR tube. Thus, any residual scandium compound on the sides of the NMR tube is not cooled and draws the ethylene out of solution by rapidly polymerizing it. Heating the upper portion of the tube with a heat gun prior to the NMR experiment effects decomposition of any residual complex on the walls and alleviates this problem.

(46) (a) Evans, J.; Schwartz, J.; Urquhart, P. W. *J. Organomet. Chem.* **1974**, *81*, C37. (b) Ikariya, T.; Yamamoto, A. *J. Organomet. Chem.* **1976**, *120*, 257.

(47) Halpern, J.; Okamoto, T. *Inorg. Chim. Acta* **1984**, *89*, L53–L54.

(48) Attempts to place the ethyl and propyl complexes on the same relative free energy scale, by equilibration together with ethylene and propylene, is of course not possible, due to the facile ethylene polymerization promoted by these compounds.

required to affix the NMR tube spinner onto the tube; the tube was then returned to the $-196\text{ }^{\circ}\text{C}$ Dewar. The sample was loaded, frozen, into the precooled NMR probe.

Ethylene Insertion Reactions: Measurement of Rate Constants Using ^{13}C NMR. The insertion rates of ethylene into the Sc–C bond of Cp^*_2ScR ($\text{R} = \text{CH}_3, \text{C}_2\text{H}_5, \text{C}_3\text{H}_7$) were measured by ^{13}C NMR (100.13 MHz) on a JEOL GX400Q spectrometer. One-pulse FT spectra were recorded automatically at preset time intervals by using a stack routine (with INIWT as the variable parameter). A heteronuclear decoupled pulse (SGBCM) was employed with a delay between pulses (92 s) of sufficient duration⁵² to enable quantitative information to be derived from relative integration of resonances of interest.⁵³ The free induction decays, measured as described above, were added together by use of an automated sequence employing the ADDBL command.^{54,55} A series of 15 FIDs were added together to produce a single spectrum; the average time for the spectrum was taken as that of the start of the accumulation of the eighth FID. By this process, approximately 35 data points could be collected from a 2-h acquisition time. The labeled resonance was integrated (relative to Cp_2Fe as an internal standard) along with the ethylene in solution. The observed rate constant was obtained from the slope of the plot of $\ln\{[\text{Cp}^*_2\text{ScR}/(\eta^5\text{-C}_5\text{H}_5)_2\text{Fe}][(\text{C}_2\text{H}_4)_t/(\text{C}_2\text{H}_4)_0]\}$ vs time. The temperature of the probe was measured after each kinetic run with a standard CH_3OH reference tube.

Kinetics of the Reaction of $\text{Cp}^*_2\text{ScCH}_3$ with 2-Butyne. Sealed NMR tube samples were prepared by dissolving $\text{Cp}^*_2\text{ScCH}_3$ (ca. 25 mg) in 0.5 mL of toluene- d_8 stock solution (with a known concentration of $(\eta^5\text{-C}_5\text{H}_5)_2\text{Fe}$ in a sealable NMR tube. The NMR tube was then attached to a calibrated gas volume. On the vacuum line, the tube was evacuated (at $-78\text{ }^{\circ}\text{C}$). 2-Butyne (ca. 10–15 equiv) was admitted to the gas bulb and condensed into the NMR tube at $-196\text{ }^{\circ}\text{C}$. The tube was sealed and stored at $-196\text{ }^{\circ}\text{C}$. The NMR probe was cooled to the desired temperature, and the sample was placed in a dry ice/acetone ($-78\text{ }^{\circ}\text{C}$) slush to thaw the solution. Just prior to loading into the precooled probe, the tube was shaken several times to effect dissolution of the butyne. Approximately 20 spectra were recorded at regular intervals over the duration of 2–3 half-lives. The temperature of the probe was measured with a CH_3OH sample after the experiment was over. Peak intensities of the $(\eta^5\text{-C}_5\text{H}_5)_2\text{Fe}$, $\text{Cp}^*_2\text{ScCH}_3$, and 2-butyne were measured for each spectrum. The observed rate constants (k_{obs}) were obtained from the slope of the plots of $\ln\{[\text{Cp}^*_2\text{ScCH}_3]/[(\eta^5\text{-C}_5\text{H}_5)_2\text{Fe}]\}$ vs time. Second-order rate constants, k_2 , were obtained by dividing the observed rate constants by the average concentration of butyne ($k_2 = k_{\text{obs}}/[2\text{-butyne}]_{\text{av}}$). Activation parameters were obtained by measuring k_2 at four different temperatures. A plot of $\ln(k_2/T)$ vs $1/T$ (T , temperature in degrees Kelvin) results in a slope of $-\Delta H^\ddagger/R$ and an intercept of $[(\Delta S^\ddagger/R) + 23.76]$. Reported errors in the rate constants represent one standard deviation from the least-squares fit of the experimental data. These errors were used in determining the uncertainty in the activation parameters.

Kinetics of $\text{Cp}^*_2\text{ScCH}_3$ with Unsymmetrical Alkynes. Samples were prepared as above except that the sealable NMR tube was fitted with a rubber septum rather than a gas volume before removing from the glovebox. The tube was cooled to $-196\text{ }^{\circ}\text{C}$ and the alkyne added via syringe. The tube was then sealed and the NMR experiment was carried out as before for 2-butyne. With unsymmetrical alkynes, two isomeric products (A, B) are formed (see eq 10 for assignment of isomers); the Cp^* peak intensities of the alkenyl complexes along with $\text{Cp}^*_2\text{ScCH}_3$ and $(\eta^5\text{-C}_5\text{H}_5)_2\text{Fe}$ were measured for each spectrum. A plot of $\ln\{[\text{Cp}^*_2\text{ScCH}_3]/[(\eta^5\text{-C}_5\text{H}_5)_2\text{Fe}]\}$ vs time again resulted in a k_{obs} which, when divided by the average concentration of alkyne, $[\text{alkyne}]_{\text{av}}$, yielded k_2 . The second-order rate constant is a sum of two rate constants for the formation of the two isomeric products, $k_2 = k_a + k_b$; the ratio of products obtained yields k_a/k_b . The isomeric products A and B were assigned by comparison with authentic samples. For example, in the reaction of $\text{Cp}^*_2\text{ScCH}_3$ and 3-phenyl-2-propyne, the two products formed are $\text{Cp}^*_2\text{ScC}(\text{CH}_3)=\text{C}(\text{CH}_3)(\text{Ph})$, A, and $\text{Cp}^*_2\text{ScC}(\text{Ph})=\text{C}(\text{CH}_3)_2$, B. Compound B was prepared independently in an NMR tube by the σ -bond metathesis reaction of $\text{Cp}^*_2\text{ScCH}_3$ and $\text{Ph}(\text{H})\text{C}=\text{C}(\text{CH}_3)_2$.

Oligomer Product Studies: Sample Preparation. The oligomerization experiments were carried out in a reaction vessel consisting of a small bulb (≈ 1 mL) connected via a short (1–2-in.) length of 6-mm tubing to

a 90° Teflon valve (Kontes or Fischer-Porter) and a 24/40 ground-glass joint. The volume of the 6-mm tubing was ≈ 1 mL. A small overhead volume was necessary to encourage condensation of ethylene. Cp^*_2ScR (typically 16–20 mg) was loaded into the vessel described above and solvent (toluene or petroleum ether, ≈ 1 mL) was distilled onto the solid. The solution was frozen at $-196\text{ }^{\circ}\text{C}$ and ethylene was condensed into the vessel from a calibrated gas volume. The solution was warmed to $-78\text{ }^{\circ}\text{C}$ in a dry ice/acetone bath and stirred for 15–45 min. Volatiles were then removed at $-78\text{ }^{\circ}\text{C}$ to a $-196\text{ }^{\circ}\text{C}$ trap and ultimately collected and measured via Toepler pump. The oligomerizations were quenched with methanol, yielding exclusively alkanes as the oligomeric products. After hydrolysis of the scandium byproducts to the oxide with water, the organic products were extracted into toluene or petroleum ether. The product solutions were dried over MgSO_4 before GC analysis.

Oligomer Product Studies: GC Analysis. The GC conditions were as follows. The injection port temperature was $430\text{ }^{\circ}\text{C}$, the detector temperature, $350\text{ }^{\circ}\text{C}$. Each run began with the oven at $80\text{ }^{\circ}\text{C}$, where it was held for 1 min. The temperature was then ramped at $10\text{ }^{\circ}\text{C}/\text{min}$ to $130\text{ }^{\circ}\text{C}$. The oven was held at this temperature for 1 min before resuming a $10\text{ }^{\circ}\text{C}/\text{min}$ ramp to $320\text{ }^{\circ}\text{C}$. A final isothermal time (typically 1–5 min) sufficient to bring about complete elution of the products was then observed. Accurate quantitative chromatography of the heavy alkanes produced in these reactions required some precautions. Specifically, the syringe needle was held in the injector port for approximately 30 s after injection to allow the needle to come to thermal equilibrium and prevent it acting as a coldfinger. If this precaution is not taken, the heavier alkanes condense onto the syringe needle and are subsequently withdrawn from the injection port, leading to anomalously and irreproducibly low integration values for the corresponding peaks in the GC trace. Quantitation of the data was performed by calculation of response factors from analysis of an external standard solution. For alkanes where no standard was available, the value of the response factor was interpolated or extrapolated.

Oligomer Product Studies: Distribution Modeling. For chain-polymerization reactions in which the initiation step is slower than the propagation step and in which the termination and chain-transfer step(s) are negligibly slow, the rate expressions governing the concentrations of the monomer and each oligomer are easily derived.⁵⁶ These assumptions were applied to the oligomerization of ethylene by $\text{Cp}^*_2\text{ScCH}_3$ and $\text{Cp}^*_2\text{ScCH}_2\text{CH}_3$, with the rate constants for initiation and propagation taken from the appropriate NMR data (vide supra). A simple BASIC program was used to express the concentration of each species as a consequence of equations in dt , the incremental time unit. Starting at $t = 0$ with a specified ratio monomer to catalyst and setting dt to a small, arbitrary value, the concentration of each species was calculated for each value of t until the concentration of monomer reached a predetermined level (based on the number of equivalents consumed in the experiment being modeled, vide supra). The calculations were then repeated with smaller values of dt until further decreases in dt affected the calculated distribution by less than 1%.

$\text{Cp}^*_2\text{ScCH}_2\text{CH}_2\text{C}_6\text{H}_5$, $\text{Cp}^*_2\text{ScCH}_3$ (0.660 g, 2 mmol) was placed in a heavy-walled glass vessel. Petroleum ether (ca. 15 mL) was condensed onto the solid and the resulting solution was cooled to $-196\text{ }^{\circ}\text{C}$. Hydrogen (1 atm) was admitted to the vessel. The solution was then stirred at room temperature for 20 min. Volatiles were removed from the bomb at $-78\text{ }^{\circ}\text{C}$. With the reaction vessel still at $-78\text{ }^{\circ}\text{C}$, degassed styrene (0.23 mL, 2 mmol) was added via syringe under an argon flush. Yellow precipitate immediately formed. Warming to room temperature effected dissolution of all the yellow solid. The solution was transferred to a frit assembly in the glovebox. Concentration of the petroleum ether and cooling to $-78\text{ }^{\circ}\text{C}$ afforded light yellow crystals of $\text{Cp}^*_2\text{ScCH}_2\text{CH}_2\text{C}_6\text{H}_5$, which were isolated by cold filtration (0.470 g, 56%). Anal. Calcd for $\text{C}_{28}\text{H}_{39}\text{Sc}$: C, 79.96; H, 9.35. Found: C, 78.75; H, 9.24.

$\text{Cp}^*_2\text{ScCH}_2\text{CHDC}_6\text{H}_5$. Deuterium (1 atm) was added to a petroleum ether solution (ca. 15 mL) of $\text{Cp}^*_2\text{ScCH}_3$ (0.440 g, 1.3 mmol) in a heavy-walled reaction vessel. After stirring the solution at room temperature for 20 min and removing the volatiles at $-78\text{ }^{\circ}\text{C}$, styrene (0.15 mL, 1.3 mmol) was added via syringe under an argon counterflow. The resulting solution was transferred to a frit assembly, which upon concentration and cooling afforded yellow crystalline $\text{Cp}^*_2\text{ScCH}_2\text{CHDC}_6\text{H}_5$ (0.245 g, 45%). Anal. Calcd for $\text{C}_{28}\text{H}_{38}\text{DSc}$: C, 79.78; H, 9.32. Found: C, 78.91; H, 9.25.

$\text{Cp}^*_2\text{ScCH}_2\text{CH}_2\text{C}_6\text{H}_4\text{-}p\text{-NMe}_2$, $\text{Cp}^*_2\text{ScCH}_3$ (0.495 g, 1.5 mmol) and $p\text{-NMe}_2\text{C}_6\text{H}_4\text{CHCH}_2$ (0.22 g, 1.5 mmol) were used as described above to produce $\text{Cp}^*_2\text{ScCH}_2\text{CH}_2\text{C}_6\text{H}_4\text{-}p\text{-NMe}_2$ (0.317 g, 46%) as a crystalline yellow solid. Anal. Calcd for $\text{C}_{30}\text{H}_{44}\text{N}_2\text{Sc}$: C, 77.72; H, 9.57; N, 3.02.

(52) A pulse delay of greater than $10T_1$ was employed to ensure complete relaxation of all ^{13}C nuclei. Values for T_1 were measured by the inversion-recovery method and analyzed by using the nonlinear least-squares method contained in the GXJEOL400 software.

(53) The NOE enhancement is expected to be equivalent for all terminal methyl groups of permethylscandocene alkyl complexes. A decoupled pulse was therefore chosen to optimize S/N.

(54) GXJEOL 400 Manual, Version GX-OPR2-3.

(55) Burger, B. J. Ph.D. Thesis, California Institute of Technology, 1987.

(56) See, for example: Allcock, H. R.; Lampe, F. W. *Contemporary Polymer Chemistry*; Prentice-Hall: Englewood Cliffs, NJ, 1981; Chapter 13, or any other basic treatment of the kinetics of ionic polymerization.

Found: C, 77.09; H, 9.37; N, 3.49.

$\text{Cp}^*_2\text{ScCH}_2\text{CH}_2\text{C}_6\text{H}_4\text{-}p\text{-CF}_3$. $\text{Cp}^*_2\text{ScCH}_3$ (0.595 g, 1.8 mmol) and $p\text{-CF}_3\text{C}_6\text{H}_4\text{CHCH}_2$ (0.32 g, 1.84 mmol) were used as described above to produce $\text{Cp}^*_2\text{ScCH}_2\text{CH}_2\text{C}_6\text{H}_4\text{-}p\text{-CF}_3$ (0.31 g, 36%), which was isolated by cold filtration. Anal. Calcd for $\text{C}_{25}\text{H}_{33}\text{F}_3\text{Sc}$: C, 71.29; H, 7.84. Found: C, 71.11; H, 7.83.

$\text{Cp}^*_2\text{ScCH}_2\text{CH}_2\text{C}_6\text{H}_4\text{-}p\text{-CH}_3$. The same procedure was used as described above, except that p -methylstyrene (0.28 mL, 2.1 mmol) was added to the petroleum ether solution of $[\text{Cp}^*_2\text{ScH}]_x$ generated from hydrogenation of 0.695 g (2.1 mmol) of $\text{Cp}^*_2\text{ScCH}_3$. Concentration and cooling of the resulting solution yielded yellow crystals of $\text{Cp}^*_2\text{ScCH}_2\text{CH}_2\text{C}_6\text{H}_4\text{-}p\text{-CH}_3$ (0.380 g, 42%). Anal. Calcd for $\text{C}_{29}\text{H}_{41}\text{Sc}$: C, 80.15; H, 9.51. Found: C, 79.90; H, 9.46.

$\text{Cp}^*_2\text{ScCH}_2\text{CH}_2\text{CH}_2\text{CH}_3$. A petroleum ether solution of $\text{Cp}^*_2\text{ScCH}_3$ (0.414 g, 1.3 mmol) was treated with H_2 as above. 1-Butene was condensed into the cooled heavy-walled reaction vessel (-196°C) from a calibrated gas volume. The resulting solution was transferred to a frit assembly. As above, repeated attempts to obtain crystals were unsuccessful. A pale yellow powder (0.165 g, 34% yield) was obtained upon removal of all volatiles. The purity of the compound was checked by ^1H NMR (>95%).

(*E*)- $\text{Cp}^*_2\text{Sc}(\text{CH}_3)\text{C}=\text{CH}(\text{CH}_3)$. A toluene solution of $\text{Cp}^*_2\text{ScCH}_3$ (369 mg, 1.12 mmol) was treated with H_2 as above. A slight excess of 2-butyne was condensed into the cooled heavy-walled reaction vessel (-196°C) from a calibrated gas volume. The resulting solution was transferred to a frit and filtered. Repeated attempts to obtain crystals were unsuccessful. An oily orange solid was obtained by removal of volatiles from a pentane solution (149 mg, 36% yield). (*E*)- $\text{Cp}^*_2\text{Sc}(\text{CH}_3)\text{C}=\text{CD}(\text{CH}_3)$ was prepared by an entirely analogous procedure, except that D_2 was used in place of H_2 . ^2H and ^1H NMR showed that deuterium was located in the vinylic position, with an incorporation of approximately 80%. In addition, some deuterium incorporation into the Cp^* rings was observed.^{17c}

Kinetics of β -Hydrogen Elimination of $\text{Cp}^*_2\text{ScCH}_2\text{CH}_2\text{R}$ Complexes.

Sealed NMR tubes were prepared and experiments were carried out as described above for the reaction of $\text{Cp}^*_2\text{ScCH}_3$ with 2-butyne. To determine the dependence of the concentration of 2-butyne on the observed rate constant, a series of experiments were carried out with $\text{Cp}^*_2\text{ScCH}_2\text{CH}_2\text{C}_6\text{H}_5$ and various concentrations of 2-butyne. Plotting the observed rate constants, k_{obs} , obtained from these experiments vs the concentration of added 2-butyne gave a line with slope 1.4×10^{-6} with deviations from the line of less than 10%. After the reaction rate was determined to be independent of 2-butyne concentration over the range 0.6–3.0 M, all subsequent kinetic runs were carried out with a butyne concentration in this range. Rate constants were obtained for each complex at several different temperatures. Activation parameters were derived from an Eyring plot as described previously.

Deuterium Kinetic Isotope Effect of β -Hydrogen Elimination. $\text{Cp}^*_2\text{ScCH}_2\text{CHDC}_6\text{H}_5$ (ca. 25 mg) was loaded into a sealable NMR tube with 0.5 mL of toluene- d_8 . A calibrated gas volume was attached to the tube. The solution was degassed at -78°C ; butyne (ca. 10 equiv) was condensed at -196°C . The tube was allowed to stand at room temperature for 5 h. The ^1H NMR spectrum (400 MHz) was recorded; the terminal vinyl resonances for styrene- d_0 and styrene- d_1 were cut from the spectrum and weighed. The isotope effect ($k_{\text{H}}/k_{\text{D}}$) was calculated from the ratio of areas of the cut and weighed peaks.

Acknowledgment. This work was supported by the USDOE Office of Basic Energy Research, Office of Basic Energy Sciences (Grant No. DE-FG03-85ER13431) and by the Shell Companies Foundation, which are gratefully acknowledged. The use of the Southern California Regional NMR Facility, supported by the National Science Foundation Grant No. CHE-84-40137 is also gratefully acknowledged. W.D.C. also thanks the National Science Foundation for an NSF Predoctoral Fellowship (1987–1990). We thank Dr. Jay A. Labinger for helpful discussions.

Oxygenation and Oxidative Coupling Processes of Alkyl Ligands of *cis*-Dialkylcobalt(III) Complexes with Dioxygen Catalyzed by Coenzyme Analogues in the Presence of Perchloric Acid

Kunio Ishikawa,^{1a} Shunichi Fukuzumi,^{*,1b} Tatsushi Goto, and Toshio Tanaka^{1c}

Contribution from the Department of Applied Chemistry, Faculty of Engineering, Osaka University, Suita, Osaka 565, Japan. Received June 27, 1989

Abstract: Oxygenation of the benzyl ligand of *cis*- $[(\text{PhCH}_2)_2\text{Co}(\text{bpy})_2]^+$ ($\text{bpy} = 2,2'$ -bipyridine) occurs efficiently in the presence of a catalytic amount of a coenzyme analogue, riboflavin, riboflavin-2',3',4',5'-tetraacetate, lumazine, or aminopterin, in acetonitrile containing perchloric acid at 298 K to produce benzyl hydroperoxide, which decomposes to yield benzaldehyde as the final oxygenated product. In the case of *cis*- $[\text{R}_2\text{Co}(\text{bpy})_2]^+$ ($\text{R} = \text{Et}, \text{Me}$), however, no oxygenation of the ligands proceeds under the same conditions; instead, oxidative coupling of the alkyl ligands of *cis*- $[\text{R}_2\text{Co}(\text{bpy})_2]^+$ takes place in the coenzyme-catalyzed oxidation by dioxygen to yield ethane and butane, respectively, when dioxygen is reduced to hydrogen peroxide. The origin of such a difference in the oxygenation and oxidative coupling pathways depending on the alkyl ligands is discussed based on the comparison of the products and kinetics with those of the one-electron oxidation of *cis*- $[\text{R}_2\text{Co}(\text{bpy})_2]^+$ by various oxidants in the absence and presence of dioxygen in acetonitrile at 298 K.

The interaction of dioxygen with transition-metal complexes has been extensively studied owing to the importance in understanding the mode of action of biological oxygen carriers.² In contrast, the contact of dioxygen with air-sensitive organometallic

compounds has usually been avoided deliberately on their handling. Thus, relatively little is known about the reactions of dioxygen with such organometallic compounds, although dioxygenation reactions of alkyl Grignard reagents have been known for a long time,³ and the chemistry of organometallic compounds containing oxo and peroxy ligands formed in the reactions with dioxygen has recently attracted increasing interest with relevance to selective catalytic oxidation processes.^{4–8} Moreover, reactions of most

(1) (a) Current address: Dental School, Tokushima University, Tokushima 770, Japan. (b) To whom correspondence should be addressed at Osaka University. (c) Current address: Department of Applied Physics and Chemistry, Fukui Institute of Technology, Fukui 910, Japan.

(2) (a) Vaska, L. *Acc. Chem. Res.* 1976, 9, 175. (b) Collman, J. P. *Ibid.* 1977, 10, 265. (c) McLendon, G.; Martell, A. E. *Coord. Chem. Rev.* 1976, 19, 1. (d) Jones, R. D.; Summerville, D. A.; Basolo, F. *Chem. Rev.* 1979, 79, 139.

(3) (a) Porter, C. W.; Steele, C. *J. Am. Chem. Soc.* 1920, 42, 2650. (b) Walling, C.; Buckler, S. A. *J. Am. Chem. Soc.* 1953, 75, 4372. (c) Walling, C.; Buckler, S. A. *Ibid.* 1955, 77, 6032.